Current Plant Biology 42 (2025) 100473

Contents lists available at ScienceDirect

Current Plant Biology

journal homepage: www.elsevier.com/locate/cpb

Physiological responses of *Lemna minor* to polystyrene and polymethyl methacrylate microplastics

Karla Košpić [a,b,1], Sandra Vitko [a,1], Luka Kobelščak [a], Ana Matešković [a], Petra Peharec Štefanić [a], Nino Dimitrov [c], Mirta Tkalec [a,*], Biljana Balen [a,*]

[a] Department of Biology, Faculty of Science, University of Zagreb, Horvatovac 102a, Zagreb 10000, Croatia
[b] Faculty of Biotechnology and Drug Development, University of Rijeka, Radmile Matejčić 2, Rijeka 51000, Croatia
[c] Croatian Institute of Public Health, Rockefellerova 7, Zagreb 10000, Croatia

ARTICLE INFO

Keywords:
Duckweed
Growth
Microplastics
Photosynthesis
Phytotoxicity
Oxidative stress

ABSTRACT

Due to its economic viability, plastic has become an indispensable material whose mass production continues to increase, raising concerns about its impact on living organisms. Its long persistence in the environment and slow degradation to microplastics (MPs) pose a serious problem, as MPs can penetrate plants and animals and interfere with physiological processes. In this study, the *in vitro* cultured duckweed *Lemna minor* was exposed to 10, 50 and 100 mg L^{-1} polystyrene (PS) and polymethyl methacrylate (PMMA) MPs for 7 days to investigate uptake and effects on growth, photosynthetic performance and oxidative stress parameters. We hypothesized that PS-MPs and PMMA-MPs would have different uptake patterns and effects on the physiology of *L. minor*, due to their different properties. A pronounced agglomeration of PMMA-MPs in the exposure medium correlated with a lower uptake of PMMA-MPs compared to PS-MPs. However, PMMA-MPs induced severe ultrastructural changes in the chloroplasts and a decrease in chlorophyll *a* and *b* content, resulting in reduced plant growth. In contrast, treatments with PS-MPs stimulated growth, especially frond area, probably as a result of increased content of photosynthetic pigments and improved photosynthetic efficiency. Both MP types induced mild oxidative stress, which triggered protective responses, but the activation of antioxidant defense was dependent on the polymer type, as PMMA-MPs slightly increased proline content and superoxide dismutase activity, while PS-MPs induced peroxidase activities. In conclusion, PS-MPs seem to be less harmful as they promote growth and photosynthetic efficiency, whereas PMMA-MPs have negative effects on *L. minor* physiology by causing structural damage to subcellular parts and inhibiting their function.

1. Introduction

According to current estimates, the human population consumes more than 400 million tons of plastic every year, mainly in the form of single-use plastic items [1]. Considering the slow rate of degradation, the sheer amount of discarded plastic and insufficient efforts to eliminate it, plastic waste continues to accumulate in various ecosystems [2] and has so far been found in terrestrial [3], freshwater [4] and marine environments [5]. In recent years, researchers have focused on a new type of plastic pollution, microplastics (MPs) – plastic particles between 1 and 1000 nm in size [6]. These microscopic fragments of various types of plastic appear to be just as ubiquitous as their larger counterparts and could pose an even greater environmental problem [1].

MPs can be divided into primary and secondary MPs depending on their origin. Primary MPs are products that are specifically manufactured at microscopic sizes, such as microbeads for cosmetic facial scrubs and abrasive particles for paint and varnish removal, while secondary MPs are produced in the environment through the degradation of larger plastic waste [7]. Although much of the research has focused on the marine environment when it comes to the presence and effects of MPs [8–11], recent studies have shown that they are also present in soil [12,13] and freshwater [14,15], including rivers, lakes, sediments, beaches,

* Corresponding authors.
E-mail addresses: karla.kospic@biotech.uniri.hr (K. Košpić), svitko@biol.pmf.hr (S. Vitko), lkobelscak@zag.aero (L. Kobelščak), amateskovic@stud.biol.pmf.hr (A. Matešković), ppeharec@biol.pmf.hr (P. Peharec Štefanić), nino.dimitrov@hzjz.hr (N. Dimitrov), mtkalec@biol.pmf.hr (M. Tkalec), bbalen@biol.pmf.hr (B. Balen).
[1] These authors contributed equally

https://doi.org/10.1016/j.cpb.2025.100473
Received 28 November 2024; Received in revised form 17 March 2025; Accepted 17 March 2025
Available online 18 March 2025

and even reservoirs, potentially contaminating drinking water sources [16]. Another concern for human health is their bioaccumulation and transfer across trophic levels, which means that MPs present in the environment could eventually be ingested by humans [17].

The basic polymer structure is one of the crucial variables in determining the degree of toxicity of MPs in exposed organisms [18], and studies have shown that the phytotoxic effects of MPs are strongly influenced by the polymer type [19–21]. The MPs most commonly identified in the environment consist of polystyrene (PS), polyethylene terephthalate (PET), polyethylene (PE), polypropylene (PP), polyvinyl chloride (PVC), polymethyl methacrylate (PMMA), polyester (PES) and polyvinyl butyral (PVB) [22,23].

In the present study, we exposed the plants separately to MPs composed of two different polymers, either PS or PMMA. Both polymers are widely distributed in freshwater environments and often originate from the degradation of larger plastic wastes, with PS being more prevalent and among the most important pollutants in aquatic and terrestrial ecosystems [24]. Previous studies have shown that PS-MPs and PMMA-MPs are frequently detected in various freshwater sources, such as rivers and lakes [25,26]. However, data on MPs contamination of aquatic ecosystems show a variable global occurrence as their distribution depends on environmental factors such as temperature, wind, rain and biofilm fixation. Available data show that PS-MPs are more than twice as abundant as PMMA-MPs in Asia and Americas (~13 % vs. ~5 %), while in Europe both MP types are equally abundant (6.98 %) [24]. Worryingly, MPs have also been found in drinking water supplies. In a study in Changsha, China, for example, MPs were detected in raw water at concentrations between 2173 and 3998 particles per liter, with both PS and PMMA among the polymers identified [27].

PS is an easily moldable and inexpensive synthetic polymer used primarily in the form of a synthetic plastic foam commonly known as Styrofoam. It is applied in the production of disposable cutlery, food and beverage containers, and insulation and packaging materials [28]. Only 10 % of PS waste is recycled annually, and PS foams are the least recycled [29], making PS one of the main pollutants in aquatic and terrestrial ecosystems [30]. As PS foam residues rapidly break down into microparticles [31], PS-MPs have become a major environmental concern in recent years due to their ability to interact with living organisms [32] and are therefore frequently investigated. Their toxic effects on humans [33,34] and animals [35,36] as well as on primary producers, algae [37,38] and plants [39,40] have already been reported. PMMA is easy to cast and manipulate and is used as a more stable substitute for glass and as a powder for casting medical prostheses and various medical devices [41]. It is also used for the production of microbeads in medicine and cosmetics [42,43]. Recycling PMMA is environmentally beneficial and economically viable [44]; however, less than 2.7 % is actually recycled [41]. Although PMMA is used in numerous commercial products, most likely leading to the formation of PMMA microplastic particles, the effects of PMMA-MPs on living organisms are poorly understood. Negative effects of exposure to PMMA-MPs have been observed in the marine diatom *Phaeodactylum tricornutum* [45], the plant *Brassica campestris* [46] and the Mediterranean mussel *Mytilus galloprovincialis* [47].

Plants are a key element in almost all ecosystems; they produce oxygen, play a role in biogeochemical nutrient cycles, serve as a food source for many species, provide hiding places and habitats, and prevent soil erosion, while humans use them for food, medicine, materials (wood, textiles), pest control and decoration [48]. It is therefore important that we understand how MPs affect them and how these effects can be mitigated. Previous studies have shown that different types of MPs can harm plants by affecting their growth and physiology [46,49–51]. However, little attention has been paid to the potential effects of MPs on aquatic plants, although their effects have been shown to depend on the properties of the plastic, the plant species and the experimental conditions [52]. In addition, the presence of MPs may affect the toxicity and bioavailability of other associated toxicants to aquatic plants [53]. *Lemna* is a genus of free-floating aquatic plants also known as duckweeds. They mostly reproduce vegetatively, which, in combination with their small size and relative ease of maintenance, makes them suitable model organisms for studying the phytotoxicity of various substances, including MPs [54]. Duckweeds, whose roots and the lower surface of the vegetative body are in direct contact with the water, can easily take up low-density MPs, such as PE, PS and PP microspheres [55], distributed in the upper layers of slow-flowing waters [56]. Rozman and Kalčíková [6] showed that tire particles, PE microbeads and PET fibers adhere to the roots of *Lemna minor* but have no effect on the specific growth rate or chlorophyll *a* content. Several studies also showed that *L. minor* tolerates adsorbed PE-MPs at moderate and high environmentally relevant concentrations without any visible effects on plant growth [57–59]. However, exposure of duckweed *Lemna minuta* to poly(styrene-co-methyl methacrylate)-MPs resulted in their adsorption on the plant surface and a negative effect on plant growth and chlorophyll content [60,61]. This demonstrates that different MP particles have significantly different pyhtotoxic effects on *L. minor* depending on their physico-chemical properties such as chemical composition, surface roughness, shape and size. Therefore, it is necessary to obtain more information on the interactions and effects of different MPs on duckweed as they play an important role in the aquatic ecosystem.

The aim of this study was to test and compare the phytotoxicity of PS-MPs and PMMA-MPs at morphological, physiological and biochemical levels in *L. minor*, to find out whether microparticles derived from different plastic polymers can have similar or different effects on the same plant species. Our hypothesis was that PS-MPs and PMMA-MPs have different uptake patterns and consequently different effects on the physiology of *L. minor*, with one type of MPs likely to cause more negative effects due to the different properties of the two polymers. To investigate the possible mechanism of toxicity induced by two types of MPs in *L. minor*, we used concentrations determined by our preliminary experiments and data from the literature [20,39,40,46] rather than those found in the natural environment. This approach allows the assessment of potential future effects, as the concentration of MPs is expected to increase in the coming years. By exploring the physiological responses and mechanisms underlying the interactions between plants and MPs, this study contributes valuable insights into the overall impact of MPs pollution on freshwater ecosystems.

2. Materials and methods

2.1. MP characterization and stability in exposure medium

Commercial monodisperse PS-MPs (mean diameter 0.147 ± 0.007 μm) and PMMA-MPs (mean diameter 0.105 ± 0.005 μm) were purchased from MicroParticles GmbH (Germany). Both types of MPs were obtained as 5 % (w/v) aqueous suspensions.

Before exposing the *L. minor* to the MPs, we tested the stability of all studied concentrations (10, 50 and 100 mg L^{-1}) of both types of microparticles in Steinberg medium [62], which was later used for the exposure experiments, at specific time intervals over a period of 7 days. The hydrodynamic diameter (d_H), which estimates the particle size, was measured with the NanoBrook 90Plus (Brookhaven Instruments, USA) using dynamic light scattering (DLS). The same instrument was used to measure the ζ-potential, which estimates the charge of the particles, at the highest concentration of each type of MPs. The results are given as mean values of 10 measurements ± standard error, and the size distributions are shown as volume distributions.

2.2. Plant material and treatments

Axenic cultures of *L. minor* L. were obtained from the established culture of the Department of Biology, Faculty of Science, University of Zagreb. In order to obtain sufficient plant material for the experiment, a modified Pirson-Seidel growth medium [63] was prepared for the propagation of the plants. The plants were grown *in vitro* for 7 days

under aseptic conditions in a growth chamber at 28 ± 3 °C with a light cycle of 16:8 h and a light intensity of 130 μmol m^{-2} s^{-1}. The plants were then transferred to Steinberg medium (pH 5.5) for acclimatization to a nutrient-poorer medium and were cultivated for a further 7 days under the same conditions. A new batch of medium was then prepared for the MPs treatment. Sterile plastic Petri dishes with a diameter of 6 cm were prepared for growth monitoring, while sterile 100 mL glass Erlenmeyer flasks were prepared for the evaluation of chlorophyll fluorescence parameters, photosynthetic pigment content and oxidative stress markers. To achieve a final MPs concentration of 10, 50 and 100 mg L^{-1}, Steinberg medium was added to each dish or flask, followed by corresponding volumes of PS-MPs or PMMA-MPs. The control plants were grown in a medium without the addition of MPs. The dishes and flasks were divided into 7 groups of 6 containers each. One colony was transferred to each dish, and several colonies were transferred to each flask and grown for a further 7 days under the same conditions.

2.3. Growth assessment

To evaluate the effects of MPs on the growth of *L. minor*, two parameters were measured – frond area and number of fronds. The total frond area was measured using the Plant Screen Mobile app [64]. Photos were taken under constant conditions in the growth chamber, with the Petri dish in the same location on the shelf and the phone positioned on two stacked boxes above the dish. The camera settings were kept constant at a resolution of 1280 × 720 with a Green Chromatic Coordinate of 0.5. The camera was calibrated with a printed checkerboard pattern (5 mm^2, 9 × 9 elements). A batch analysis of all photos was performed, with two images per sample: one on the day of planting (day 0) and another on the final day of treatment. The following analysis parameters were used: Method – Greenness (threshold: 0.50), minimum hole size 1, minimum object size 1, and the option "Calculate Metric Values" was selected as yes. The change in frond area was calculated by subtracting the values from day 0 values from the final day's values. The number of fronds was counted daily, and the growth rate based on the number of fronds was calculated using the following formula [65]:

$$\text{Growth rate} = \frac{\ln(N_{tx}) - \ln(N_{ty})}{t_x - t_y},$$

where $\ln(N_{tx})$ represents the natural logarithm of the number of fronds at time t_x, and $\ln(N_{ty})$ is the natural logarithm of the number of fronds from the previous day (t_y). The difference is divided by the time interval between t_x and t_y. This calculation was repeated for each day over the course of 7 days and averaged for each biological replicate to determine the overall growth rate of frond numbers over a period of 7 days.

2.4. MP uptake and accumulation

After harvesting, the fronds were thoroughly washed with ultrapure water to remove adhering MPs. The tissue was then frozen in liquid nitrogen and lyophilized at −64 °C and 0.025 mbar for 24 h.

The detection and quantification of MPs was carried out by pyrolysis gas chromatography/mass spectrometry (Py-GC/MS). Prior to Py-GC/MS analysis in the inert stainless-steel cup, 0.4 mg of the lyophilized plant sample was weighed on the Mettler Toledo XPR 226CDR microbalance. Subsequently, 4.0 mg of $CaCO_3$ was added to the sample cup and placed onto auto-shot sampler (AS-1020E, Frontier Laboratories) for pyrolysis. The auto-shot sampler, as part of the equipment of the microfurnace pyrolyzer (EGA/Py3030D, Frontier Laboratories Europe, Essen, Germany), was directly connected to the GC/MS instrument (Shimadzu QP2010 Plus, Shimadzu Japan) via the split/splitless injection port. Pyrolysis was carried out at 600 °C, while the interface temperature was kept at 300 °C. The carrier gas was helium (99.999 % purity) at a pressure flow control rate of 75 kPa, and the injection was split 1:50 at 300 °C. The GC injection port was connected to a quadrupole mass detector via a column system consisting of a precolumn (Ultra ALLOY+-50, 2 m × 0.25 mm i.d., coated with 1.0 μm film thickness of 50 % diphenyl and 50 % dimethylpolysiloxane) (Frontier Laboratories, Ltd.), a separation column (Ultra ALLOY+-5, 30 m × 0.25 mm i.d., coated with 0.5 μm film thickness of 5 % diphenyl and 95 % dimethylpolysiloxane) (Frontier Laboratories, Ltd.) and a vent-free GC/MS adapter. The chromatography program was: initial temperature 40 °C (hold for 2 min) → 280 °C (20 °C min^{-1}, hold for 10 min) → 320 °C (40 °C min^{-1}, hold for 20 min). The ion source of the mass spectrometer was kept at 250 °C. Electron ionization (EI) mass spectra of 70 eV were recorded in the range of *m/z* 29–350 amu. Polymer mixtures of 12 polymers with the characteristic ions of 2,4,6-triphenyl-1-hexene (styrene trimer) (SSS) *m/z* 91 and for methyl methacrylate (MMA) *m/z* 100 were used to validate a calibration curve for the quantification of MPs in plants. A MPs standard calibration set (Frontier Laboratories Ltd., Japan) with MPs and F-Search MPs 2.1 software (Frontier Laboratories, Ltd.) was used. Quality control parameters were the correlation coefficient of the linear calibration curve of more than 0.99 with a probability of more than 90 % and the RSD% value of the measured samples.

2.5. Chlorophyll fluorescence induction curve (OJIP) and photosynthetic pigments

After the plants from the flasks had been washed with distilled water, they were transferred to plastic trays previously lined with moistened filter paper, one tray for each of the 7 groups. Six coin-sized circles were drawn on each filter paper, and each circle was filled with *L. minor* colonies to cover the surface, with one circle per flask/replicate. The trays were then covered and placed in a dark room at 24 °C for 30 min to allow the photosystem II (PSII) reaction centers to fully oxidize and minimize fluorescence. Chlorophyll *a* fluorescence was measured using a FluorPen FP100 fluorimeter (Photon Systems Instruments, Czech Republic). The plants were illuminated with a blue light pulse (λ = 455 nm, photon flux density = 3000 μmol m^{-2} s^{-1}) and the fluorimeter recorded the fluorescence intensities at 50 μs (F_0), 2 ms (F_J), 30 ms (F_I) and the maximum fluorescence intensity (F_m). The JIP-test [66] was used to analyze the original data and calculate fluorescence parameters, including the maximum quantum yield of PSII (F_V/F_M) and the photosynthetic performance index (PI_{ABS}). In addition, specific energy flux parameters (ABS/RC – photon absorption per active reaction center, TR_0/RC – photon capture rate per active reaction center, ET_0/RC – electron transfer per active reaction center, and DI_0/RC – energy dissipation per active reaction center) were analyzed to evaluate the energy dynamics within PSII reaction centers, along with RC/CS_o to determine the density of active reaction centers per excited cross-section.

Approximately 30 mg of frozen plant material (stored at −80 °C) was homogenized with 10 mg of $CaCO_3$ and 1 mL of cold 80 % (v/v) acetone to extract photosynthetic pigments. The obtained extracts were vortexed for 10 seconds and centrifuged at 5000 × *g* for 10 min at 4 °C. The supernatant was collected, and the remaining sediment was washed twice with cold acetone, vortexed and centrifuged again. The supernatant from the first extraction and subsequent washes were combined and the total volume was adjusted to 1.5 mL with cold acetone. The absorbance was measured at 470, 645 and 663 nm. The concentrations of chlorophyll *a*, chlorophyll *b* and total carotenoids were calculated and expressed in μg mg^{-1} of fresh weight [67]

2.6. Leaf ultrastructure and anatomy

For TEM analysis, the small pieces of *L. minor* fronds were fixed with pre-cooled 1 % glutaraldehyde in 0.5 M cacodylate buffer (pH 7.2) for 1 hour in an ice bath. Samples were then washed twice with cold 0.5 M cacodylate buffer for 10 min and post-fixed in an ice bath with 1 % osmium tetroxide in the same buffer for 1 h, followed by 10 washes in cold distilled water. Dehydration was carried out with a series of increasing ethanol concentrations (50, 60, 70, 80 and 96 %), with each

concentration acting for 10 min. Finally, the material was soaked overnight in absolute ethanol. The next day, the material was placed in a mixture of absolute ethanol and 100 % acetone for 30 min, followed by additional 30 min in 100 % acetone. The material was then placed in a mixture of Spurr's medium and acetone, first in one part Spurr's/two parts acetone for 30 min, then in one part Spurr's/one part acetone for a further 30 min and finally in two parts Spurr's/one part acetone for 30 min. The material was then placed in Spurr's medium at 45 °C for 2 h. Finally, the material was placed in a plastic mold and polymerized in Spurr's medium at 65 °C for 48 h. Ultrathin sections were made using the ultramicrotome (MT6000 XL, RMC Inc., SAD). The sections were contrasted with Uranyless aqueous solution (em-grade, France) for 10 min and then with 3 % lead citrate (em-grade, France) for further 10 min. The ultrathin sections were analyzed with the FEI Morgagni 268D transmission electron microscope at 70 kV.

2.7. Detection of large subunit of RuBisCO (rbcL)

Proteins were extracted with Tris-HCl buffer (pH 8.0) containing 0.5 M sucrose, 6.5 mM dithiothreitol and 8.25 mM cysteine-HCl. Samples were homogenized with polyvinylpolypyrrolidone, centrifuged at 20,000 × g at 4 °C for 30 min, and the supernatant was collected. Protein concentration was determined by Bradford assay [68] using the standard curve prepared with known concentrations (0.2 – 2.0 mg mL^{-1}) of bovine serum albumin (BSA) in Tris-HCl buffer, pH 8.0. Proteins were denatured by mixing with Laemmli sample buffer (87.5 mM Tris-HCl, pH 6.8, 2 % (w/v) sodium dodecyl sulfate, 45 % (v/v) glycerol, 12.5 % (v/v) 2-mercaptoethanol, 0.0125 % (w/v) bromophenol blue) and heated at 95 °C for 5 min. Equal amounts of protein were separated by SDS-PAGE (12 % resolving gel, 4 % stacking gel) and transferred to a 0.45 μm nitrocellulose membrane using a wet transfer system at 60 V for 60 min. The efficiency of the transfer was checked by Ponceau S staining. Membranes were blocked for 1 h at room temperature with 5 % (w/v) nonfat milk in 1 × Tris-buffered saline containing 1 % (v/v) Tween® 20 detergent (TBS-T) and then incubated overnight at 4 °C with primary anti-rbcL antibody (1:4000 in blocking solution). After washing twice in 1 × TBS-T for 5 min, the membranes were incubated with HRP-conjugated secondary antibody (1:10,000) for 1 h at room temperature. Detection was performed with chemiluminescent substrate (Immobilon Forte Western HRP, Merck Millipore) and imaged using the C-DiGit Blot Scanner (LI-COR Biosciences, USA). The band intensity was quantified using Image Studio™ Lite 5.2 software.

2.8. Extraction of total soluble proteins

To isolate the total soluble proteins, mechanical lysis was performed using a pre-cooled mortar and pestle. Specifically, 80 mg of lyophilized tissue was crushed with the addition of 50 mg of insoluble polyvinylpyrrolidone (PVP) and homogenized in 1 mL of 0.1 M potassium phosphate buffer, pH 7.0. The resulting homogenates were centrifuged at 20,000 × g at 4 °C for 45 min, and the supernatant was transferred to clean tubes. The concentration of total proteins in each sample was determined by Bradford assay [68] using the standard curve prepared with known concentrations (0.2 – 2.0 mg mL^{-1}) of BSA in 0.1 M potassium phosphate buffer, pH 7.0. Measurements were performed with a Specord 50 PLUS (Analytik Jena, Germany) spectrophotometer. The remaining aliquots of protein extracts were stored at −20 °C until they were used for the determination of protein carbonyl content and enzymatic activities.

2.9. Determination of H_2O_2 content

To determine the content of hydrogen peroxide (H_2O_2), we used the modified method of Mátai and Hideg [69], which is based on the oxidation of ferrous ions in the ferrous oxidation-xylenol orange (FOX) reagent by H_2O_2, with the absorbance measured at 560 nm. A total of 80 mg of fresh plant tissue was snap-frozen in liquid nitrogen, transferred to clean tubes, mixed with 500 μL of 70 % (v/v) ethanol and extracted using a mechanical homogenizer (Mixer Mill MM 200, Retsch, Germany) at a speed of 30 Hz at room temperature. The homogenates were centrifuged at 20,000 × g for 10 min at 4 °C. An aliquot of 100 μL of each sample was mixed with 1000 μL FOX reagent (124 μM xylenol orange, 99 mM sorbitol and 0.248 mM $(NH_4)_2Fe(SO_4)_2 \times 6\ H_2O$ in 2.5 M H_2SO_4) and incubated for 15 min at room temperature in the dark. The absorbance was measured spectrophotometrically at 560 nm, and the H_2O_2 concentration in the samples was determined using the standard curve prepared with H_2O_2 standard solutions (1.82 – 72.8 μM); the results were expressed as % of control.

2.10. Malondialdehyde and protein carbonyl content

The level of lipid peroxidation was determined indirectly by measuring the content of one of the predominantly formed products, malondialdehyde (MDA), according to the modified method of Heath and Packer [70]. A total of 50 mg of frozen tissue was homogenized in 1 mL of 0.3 % (w/v) 2-thiobarbituric acid (TBA) prepared in 10 % (w/v) trichloroacetic acid (TCA) and incubated at 95 °C for 30 min. The mixtures were cooled in an ice bath and then centrifuged at 20,000 × g at 4 °C for 1 h. The absorbance of the supernatant was measured spectrophotometrically at 532 nm and 600 nm, with the difference between these two values representing a correction for non-specific turbidity. The MDA content was calculated using the molar absorption coefficient of 155 $mM^{-1}\ cm^{-1}$ and expressed in nmol g^{-1} of fresh weight.

A modified method by Levine et al. [71] was used to determine the protein carbonyl content. The principle is based on the derivatization of the carbonyl group with 2,4-dinitrophenylhydrazine (DNPH), resulting in a colored dinitrophenylhydrazone adduct whose absorbance is measured spectrophotometrically [72]. For this purpose, 200 μL of protein extracts (Section 2.8) were mixed with 300 μL of 10 mM DNPH prepared in 2 M HCl and incubated for 1 h in the dark at room temperature with occasional shaking. After incubation, the proteins were precipitated by adding 500 μL of 10 % (w/v) TCA and incubated again at −20 °C for 5 min, followed by centrifugation at 20,000 × g for 10 min at 4 °C. After discarding the supernatant, the pellets were washed three times in 500 μL of ethanol/ethyl acetate 1:1 (v/v) to remove unbound DNPH. The pellets were then reconstituted in 1 mL of 6 M urea in 20 mM potassium phosphate buffer, pH 2.4, by vortexing and brief incubation in an ultrasonic bath. The absorbance was measured spectrophotometrically at 370 nm against the reference prepared for each sample in 2 M HCl without DNPH. The absorbance of each sample was also measured at 280 nm and 260 nm to estimate protein recovery and DNA contamination, respectively. The standard curve was prepared from BSA standards (0.2 – 2.0 mg mL^{-1}) dissolved in 6 M urea in 20 mM potassium phosphate and measured at 280 nm. The molar absorption coefficient of the aliphatic hydrazone of 22 $mM^{-1}\ cm^{-1}$ was used to calculate the carbonyl content of the proteins. The results were expressed in μmol mg^{-1} of protein.

2.11. Determination of proline content

The protocol according to Bauer et al. [73] was used to determine the content of a non-enzymatic antioxidant proline. A total of 500 μL of 70 % (v/v) ethanol and a small amount of PVP were added to 50 mg of previously frozen tissue and homogenized in a mechanical homogenizer at room temperature and a speed of 30 Hz for 3 × 4 min each. The homogenates were centrifuged for 45 min at 20,000 × g and 4 °C. A total of 200 μL of the supernatant was added to 800 μL of the reaction mixture (1 % (w/v) ninhydrin, 60 % (v/v) acetic acid and 20 % (v/v) ethanol) and heated in a thermomixer at 95 °C for 20 min. The mixtures were then cooled in an ice bath and centrifuged at 20,000 × g for 1 min. The absorbance values of the supernatants were measured spectrophotometrically at 520 nm, and the proline concentration was determined

using a standard curve prepared from proline standards of known concentrations (0.04 – 1 mM) in 70 % (v/v) ethanol. The results were expressed in μmol g^{-1} of fresh weight.

2.12. Antioxidant enzymes activity assays

The activity of superoxide dismutase (SOD) (EC 1.15.1.1) was determined according to the method published by Beauchamp and Fridovich [74], which is based on a photochemical reaction in which riboflavin generates a superoxide radical ($O_2^{\bullet -}$) and thereby reduces nitroblue tetrazolium (NBT) to a purple-colored product – formazan. The color change is measured spectrophotometrically at 560 nm and the SOD activity is determined using a standard curve prepared from SOD standard solutions (0.025 – 1 U μL^{-1}). Since one unit (U) of SOD is defined as the amount of enzyme required for 50 % inhibition of NBT reduction, we first measured the maximum absorbance resulting from a reaction of riboflavin with the reaction mixture in the absence of SOD (i.e., without addition of protein extracts). A total of 800 μL of the reaction mixture (13 mM methionine, 75 μM NBT and 0.1 M ethylenediaminetetraacetic acid (EDTA)) was mixed with 180 μL of potassium phosphate buffer, pH 7.8, and 20 μL of 2 mM riboflavin was added. The absorbance was measured after an 8-min incubation in a cuvette exposed to light (15 W), and the same mixture, which was not exposed to light, served as a reference. To measure absorbance in protein extracts (Section 2.8), the volume of protein extract from the control samples was added, resulting in a 50 % decrease in absorbance, and the volume of the remaining samples was adjusted accordingly. The results were expressed as U of SOD activity mg^{-1} of the proteins.

Catalase activity (CAT) (E.C. 1.11.1.6) was determined according to the method of Aebi et al. [75] based on the observation of the degradation of H_2O_2, as indicated by a decrease in absorbance measured at 240 nm. A total of 50 μL of the protein extract (Section 2.8) was mixed with 950 μL of the reaction mixture (10 mM H_2O_2 and 50 mM potassium phosphate buffer, pH 7.0). The absorbance was measured every 10 s for one min. CAT activity was calculated using a molar extinction coefficient of 36 mM^{-1} cm^{-1} and expressed as μM of decomposed H_2O_2 min^{-1} mg^{-1} of protein.

The activity of pyrogallol peroxidase (PPX) (EC 1.11.1.7) was evaluated as described by Nakano and Asada [76]. The method is based on the measurement of the increase in absorbance at 430 nm due to the oxidation of pyrogallol to purpurogallin in the presence of H_2O_2. A total of 20 μL of protein extract (Section 2.8) was added to 980 μL of the reaction mixture (50 mM potassium phosphate buffer, pH 7.0, 20 mM pyrogallol and 1 mM H_2O_2), after which the absorbance was measured every 15 s over a period of two min. A molar extinction coefficient of 2.6 mM^{-1} cm^{-1} was used to calculate PPX activity, which was expressed as μmol of purpurogallin min^{-1} mg^{-1} of protein.

The method published by Nakano and Asada [76] was used to determine the activity of ascorbate peroxidase (APX) (EC 1.11.1.11). A total of 180 μL of the protein extract (Section 2.8) was mixed with 800 μL of the reaction mixture (50 mM potassium phosphate buffer, pH 7.0, and 10 mM EDTA), 10 μL of 0.1 mM ascorbic acid and 10 μL of 12 mM H_2O_2. The decrease in absorbance resulting from ascorbate oxidation was measured every 15 s over a period of two min at 290 nm. Subsequently, the specific APX activity was calculated based on the molar extinction coefficient of 2.8 mM^{-1} cm^{-1} and expressed as μmol of oxidized ascorbate min^{-1} mg^{-1} of protein.

2.13. Statistical analysis

The results are presented as the mean value of at least 5 replicates ± standard error. The effect sizes were estimated using η^2 for comparisons between control and PS- or PMMA-treated plants and Cohen's d for pairwise comparisons between PS and PMMA. η^2 values of 0.01 – 0.05 indicate a small effect, 0.06 – 0.13 a medium effect and ≥ 0.14 a large effect. For Cohen's d, values between 0.2 – 0.49 stand for a small effect, 0.5 – 0.79 for a medium effect and ≥ 0.8 for a large effect [77]. For the statistical analysis of d_H and ζ-potential, a one–way ANOVA followed by Duncan's Multiple Range and Critical Ranges post hoc test was used, while for all other parameters Fisher's Least Significant Difference (LSD) post hoc test was used to compare different concentrations of the same MP treatment with the control group. Student's *t*-test was used to compare the same concentrations of PS-MPs and PMMA-MPs. Statistical significance was considered at $p \leq 0.05$. Statistical analyses were performed with Statistica 14.0 (TIBCO Software Inc., SAD).

3. Results

3.1. MP characterization and stability in exposure medium

The dispersion system used in this study was the Steinberg medium (Section 2.1). The temporal evolution of the d_H of PS-MPs and PMMA-MPs after addition to the Steinberg medium is shown in Table 1.

For 10 mg L^{-1} PS-MPs, the DLS measurements showed a gradual agglomeration of the particles. At the beginning of the exposure, the size of the MPs was similar to that in pure water with a low PDI, indicating highly monodisperse (uniform) particles. From day 1 to day 4, a significant increase ($p \leq 0.05$) in size and PDI values was observed,

Table 1
Temporal analysis of changes in hydrodynamic diameter (d_H), expressed as intensity distributions and polydispersity index (PDI), of 10, 50 and 100 mg L^{-1} PS-MPs and PMMA-MPs in Steinberg nutrient medium over a period of 7 days.

PS-MPs (mg L^{-1})						
Time	10		50		100	
	d_H (nm)	PDI	d_H (nm)	PDI	d_H (nm)	PDI
0 min	156.02 ± 1.84^{d}	0.086	147.08 ± 2.09^{a}	0.034	142.48 ± 1.36^{ab}	0.076
day 1	170.60 ± 2.19^{bc}	0.146	149.41 ± 1.86^{a}	0.043	145.66 ± 1.40^{ab}	0.005
day 2	174.02 ± 1.83^{b}	0.186	148.47 ± 1.62^{a}	0.005	144.82 ± 2.23^{ab}	0.043
day 4	191.56 ± 3.33^{a}	0.152	145.63 ± 1.88^{a}	0.005	143.43 ± 2.15^{ab}	0.005
day 7	143.35 ± 6.68^{e}	0.477	120.40 ± 1.79^{b}	0.005	143.21 ± 1.80^{ab}	0.005
PMMA-MPs (mg L^{-1})						
Time	10		50		100	
	d_H (nm)	PDI	d_H (nm)	PDI	d_H (nm)	PDI
0 min	130.00 ± 1.84^{b}	0.193	133.30 ± 3.54^{cd}	0.212	114.52 ± 0.77^{e}	0.077
day 1	128.49 ± 0.94^{b}	0.063	136.81 ± 0.59^{c}	0.061	127.29 ± 1.18^{d}	0.053
day 2	124.86 ± 0.74^{b}	0.125	145.68 ± 2.61^{b}	0.109	138.88 ± 1.42^{c}	0.103
day 4	122.43 ± 1.60^{b}	0.005	139.78 ± 1.33^{bc}	0.096	156.65 ± 2.41^{b}	0.055
day 7	796.18 ± 94.78^{a}	0.437	164.29 ± 2.73^{a}	0.344	191.51 ± 3.37^{a}	0.087

suggesting moderate polydispersion of particles and partial agglomeration. However, on day 7, the d_H values were significantly lower ($p \leq 0.05$) than at the beginning of the measurements, but at the same time showed a high PDI value, indicating a breakdown of agglomerates and dispersion of particles with broad or multimodal sizes. At higher PS-MP concentrations, a significant decrease in size with low PDI values was observed at the end of the exposure, indicating smaller monodisperse particles, while at the highest concentration, no statistically significant changes in d_H values were observed at any time point (Table 1).

In contrast to PS-MPs, PMMA-MPs at 10 mg L^{-1} showed a significant increase in d_H ($p \leq 0.05$) only at the last measured time point (day 7), which was also accompanied by a high PDI value, indicating the formation of agglomerates and the dispersion of particles of broad or multimodal size. At concentrations of 50 and 100 mg L^{-1}, a significant ($p \leq 0.05$) shift in particle sizes to higher values was observed over time. However, an increase in the PDI value was only observed at the 50 mg L^{-1} treatment, indicating a moderate polydispersion of MP sizes, while the PDI value remained low at the highest concentration tested, which together with the increase in d_H could indicate a slight but stable agglomeration (Table 1).

The ζ-potential of the 10 mg L^{-1} PS-MPs dispersion was negative from the beginning of the measurements and increased only slightly and gradually in the Steinberg medium. At the higher concentrations, a more pronounced increase in the negative charge of the MPs was already observed on day 1 compared to the initial values, which was significant at 100 mg L^{-1} ($p \leq 0.05$). However, at 50 mg L^{-1} the ζ-potential remained stable until the end of the experiment, while at 100 mg L^{-1} it increased with time and reached the most negative value on day 7 (Table 2).

As for the PMMA-MPs, the particles became more negatively charged at the 10 mg L^{-1} concentration from the day 1 and remained stable until the end of the experiment. The treatments with 50 mg L^{-1} resulted in a gradual and significant ($p \leq 0.05$) increase in the negative charge of the particles from day 1 to day 4; however, on day 7, the negative charge of the ζ-potential decreased significantly ($p \leq 0.05$). The negative charge of the 100 mg L^{-1} PMMA-MPs measured at 0 minute became slightly more negative on days 1, 4 and 7, respectively, while a significant ($p \leq 0.05$) shift to a positive ζ-potential was observed at the end of the experiment (Table 2).

3.2. Growth parameters

The 7-day growth of *L. minor* in Steinberg medium containing PS-MPs or PMMA-MPs showed different effects on frond area (Fig. 1A). PS-MPs did not significantly alter frond area at any concentration compared to the control group, although a strong positive effect was observed ($\eta^2 = 0.14$). Plants exposed to a concentration of 10, 50 and 100 mg L^{-1} showed an increase in frond area of 36 %, 41 % and 22 %, respectively, compared to the control group. Conversely, PMMA-MPs showed a moderate effect in reducing frond area ($\eta^2 = 0.12$). In addition, plants exposed to the highest concentration, i.e. 100 mg L^{-1}, had a significantly ($p \leq 0.05$) smaller frond area than plants exposed to the

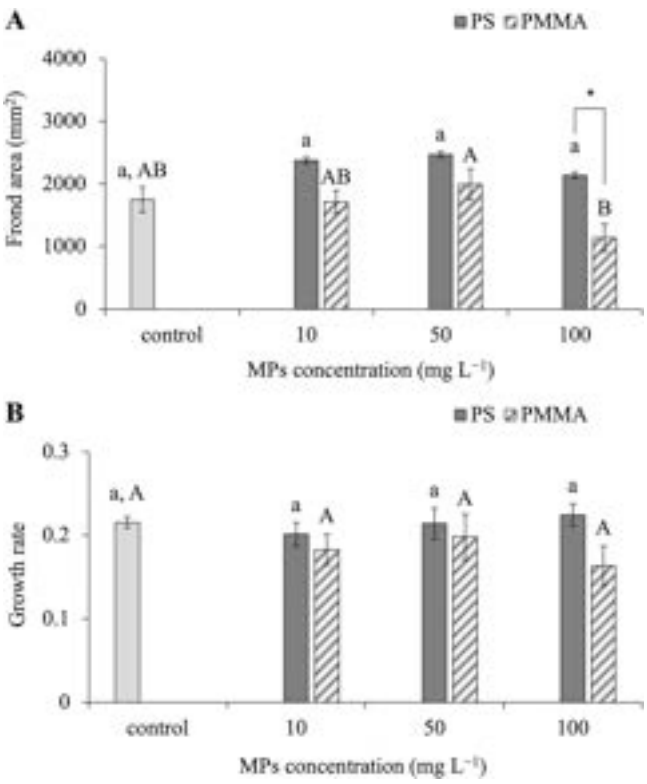

Fig. 1. Frond area (A) and growth rate based on the frond number (B) of *L. minor* plants grown for 7 days in Steinberg nutrient medium supplemented with PS-MPs or PMMA-MPs in concentrations 10, 50, or 100 mg L^{-1}. Control plants were grown in medium without MPs. Results are shown as the average value of 5–6 biological replicates and bars represent standard error. Different lowercase letters indicate a significant difference between control and PS-MP-treated plants, while different uppercase letters indicate a significant difference between control and PMMA-MP-treated plants (one-way ANOVA, followed by post hoc LSD test, $p \leq 0.05$). Asterisks indicate a significant difference between two different MP types at the same concentration (Student's *t*-test, $p \leq 0.05$).

50 mg L^{-1} concentration and a 35 % smaller frond area compared to the control group. A comparison between PS-MPs and PMMA-MPs at the same concentrations showed a strong difference between the two microplastics ($d > 0.9$). A significant difference ($p \leq 0.05$) was observed at 100 mg L^{-1}, with plants exposed to PS-MPs showing a larger frond area than those exposed to PMMA-MPs. The change in the number of fronds of *L. minor* over a 7-day period, expressed as growth rate, was not significantly ($p \leq 0.05$) affected by either type of MPs at any concentration (Fig. 1B). However, plants exposed to 100 mg L^{-1} PMMA-MPs had a 24 % lower growth rate than control plants and a 27 % lower growth rate than PS-treated plants, and this inhibitory effect showed a large effect size ($\eta^2 = 0.16$ and $d = 1.3$, respectively).

Table 2
Temporal analysis of changes in zeta (ζ) potential (mV) of 10, 50 and 100 mg L^{-1} PS-MPs and PMMA-MPs in Steinberg nutrient medium over a period of 7 days.

PS-MPs (mg L^{-1})				PMMA-MPs (mg L^{-1})		
Time	10	50	100	10	50	100
0 min	-25.21 ± 1.21^{a}	-16.66 ± 10.28^{a}	-17.38 ± 3.50^{a}	-18.47 ± 0.18^{a}	-18.87 ± 2.90^{b}	-25.80 ± 1.97^{b}
day 1	-28.77 ± 1.63^{a}	-33.05 ± 1.65^{ab}	-36.30 ± 0.98^{b}	-28.83 ± 3.46^{b}	-27.87 ± 1.50^{bc}	-30.78 ± 0.92^{b}
day 2	-29.62 ± 2.28^{a}	-38.22 ± 2.29^{b}	-40.02 ± 1.88^{bc}	-29.94 ± 4.31^{b}	-35.18 ± 3.66^{c}	-31.58 ± 0.01^{b}
day 4	-29.95 ± 1.88^{a}	-34.84 ± 3.42^{b}	-38.17 ± 1.58^{b}	-22.56 ± 3.86^{b}	-34.09 ± 3.23^{c}	-31.88 ± 4.44^{b}
day 7	-31.92 ± 2.68^{a}	-37.37 ± 0.97^{b}	-47.66 ± 3.83^{c}	-20.86 ± 9.88^{b}	-4.46 ± 5.76^{a}	1.20 ± 0.77^{a}

Table 3
The uptake of MPs in *L. minor* plants grown for 7 days in Steinberg nutrient medium supplemented with PS-MPs or PMMA-MPs in concentrations 10, 50, or 100 mg L^{-1}. Control plants were grown in medium without MPs. Results are shown as the average value of 3 biological replicates ± standard error.

MP concentration (mg L^{-1})	MP type	
	PS-MPs	PMMA-MPs
	MP content (μg MPs/ 0.4 mg lyophilized tissue)	
0 (control)	0.380 ± 0.009	0.000 ± 0.000
10	0.921 ± 0.009	0.568 ± 0.046
50	1.917 ± 0.162	1.510 ± 0.167
100	2.303 ± 0.149	1.720 ± 0.121

3.3. MP uptake and accumulation

The uptake of PS-MPs and PMMA-MPs by *L. minor* plants was analyzed by Py-GC-MS to verify whether fronds can accumulate microparticles based on certain types of plastic polymers.

After treatment with PS-MPs, a clear linear increase in styrene content with increasing treatment concentration was observed in the fronds of *L. minor* (Table 2), which was based on the appearance of a peak typical of the styrene trimer of 2,4,6-triphenyl-1-hexene (SSS), *m/z* 91 (Supplementary Fig. 1). However, a small SSS peak was also observed in the fronds of the control group that was not treated with PS-MPs, although it was much less pronounced compared to the standard and treatments (Table 2).

The treatments with PMMA-MPs also led to an accumulation of microplastic particles based on the characteristic monomer peak of methyl methacrylate (MMA) *m/z* 100 (Supplementary Fig. 2), although the differences in the amount of accumulated MMA between the concentrations of 50 and 100 mg L^{-1} were not as pronounced as in the treatments with PS-MPs.

It can also be observed that more styrene than MMA accumulated in the fronds of *L. minor* at the same treatment concentration (Table 3). When comparing the uptake of microparticles at equal concentrations of PS-MPs and PMMA-MPs, the greatest difference in accumulation occurred at the lowest concentration (10 mg L^{-1}), with a variation of 38 %. In contrast, the differences in microparticle accumulation at higher concentrations (50 and 100 mg L^{-1}) were smaller and more consistent, with variations of 21 % and 25 %, respectively.

3.4. Photosynthetic parameters

Exposure of *L. minor* to PS-MPs and PMMA-MPs resulted in remarkable changes in photosynthetic parameters and pigment content (Table 4). Large positive effects of PS-MPs on F_V/F_M ($\eta^2 = 0.24$) and PI_{ABS} ($\eta^2 = 0.35$) were observed compared to the control. Moreover, the increase was statistically significant ($p \leq 0.05$) for F_V/F_M of plants exposed to 10 mg L^{-1} PS-MPs and for PI_{ABS} of plants exposed to 10 and 50 mg L^{-1}. In contrast, PMMA-MPs had a small effect ($\eta^2 = 0.05$) on F_V/F_M, but a large and positive effect ($\eta^2 = 0.35$) on PI_{ABS}. A significant ($p \leq 0.05$) increase in PI_{ABS} values was observed at 50 mg L^{-1}. When comparing the effects of PS-MPs and PMMA-MPs, a large effect size ($d > 1.2$) was found for 10 and 50 mg L^{-1} concentrations. Plants exposed to 10 mg L^{-1} PS-MPs had significantly ($p \leq 0.05$) higher F_V/F_M and PI_{ABS} values and those exposed to 50 mg L^{-1} PS-MPs had significantly ($p \leq 0.05$) higher PI_{ABS} values.

Analysis of energy dynamics within PSII reaction centers showed that plants treated with both PS-MPs and PMMA-MPs had lower photon absorption (ABS/RC), photon capture rate (TR_0/RC) and energy dissipation (DI_0/RC) per active reaction center, although the effect size was larger ($\eta^2 > 0.14$) for PS-MPs treatments. Electron transfer per active reaction center (ET_0/RC) and the active reaction center density per excited cross-section (RC/CS_o) increased after treatments with both MPs, showing a large effect size ($\eta^2 > 0.14$) (Supplementary Fig. 3).

Chlorophyll *a* (Chl *a*) and chlorophyll *b* (Chl *b*) content followed a similar pattern, with PS-MPs having a large positive effect compared to the control ($\eta^2 = 0.51$). Plants exposed to 10 mg L^{-1} PS-MPs had a 20 % higher Chl *a* content than the control group. In addition, exposure to PS-MPs at 50 mg L^{-1} significantly ($p \leq 0.05$) increased both Chl *a* and Chl *b* compared to the control group and the highest PS-MPs concentration (Table 4). In contrast, PMMA-MPs had a large negative effect compared to the control ($\eta^2 = 0.21$). Plants exposed to 10 mg L^{-1} PMMA-MPs had 24 % and 22 % lower Chl *a* and Chl *b* content, respectively. In addition, plants exposed to 10 and 50 mg L^{-1} PMMA-MPs had significantly ($p \leq 0.05$) lower Chl *a* and Chl *b* contents than those exposed to PS-MPs. The content of carotenoids (Cars) showed a similar trend, with a significantly ($p \leq 0.05$) higher content in plants exposed to 10 and 50 mg L^{-1} PS-MPs than in the control. Interestingly, plants exposed to 50 mg L^{-1} PS-MPs also had a significantly ($p \leq 0.05$) higher Cars content than plants exposed to the same concentration of PMMA-MPs, while plants exposed to 100 mg L^{-1} PS-MPs had a significantly ($p \leq 0.05$) lower Cars content than plants exposed to 100 mg L^{-1} PMMA-MPs.

In plants exposed to PS-MPs, the relative intensity of the large subunit of RuBisCO (rbcL) remained comparable to the control, especially in plants exposed to 10 and 50 mg L^{-1} PS-MPs, which showed a decrease of about 5–15 % (Supplementary Fig. 4). Plants exposed to 100 mg L^{-1} PS-MPs showed a decrease of about 35 %. Exposure to PMMA-MPs resulted in a substantial decrease in rbcL intensity. Treatment with 10 mg L^{-1} PMMA-MPs resulted in a reduction of about 70 % compared to the control, while treatments with 50 and 100 mg L^{-1} showed a reduction of about 55 % and 45 %, respectively.

Table 4
Photosynthetic parameters maximum quantum yield – F_V/F_M, performance index – PI_{ABS} as well as content of chlorophyll *a* – Chl *a*, chlorophyll *b* – Chl *b* and total carotenoids – Cars of *L. minor* plants grown for 7 days in Steinberg nutrient medium supplemented with PS-MPs or PMMA-MPs in concentrations 10, 50, or 100 mg L^{-1}. Control plants were grown in medium without PS-MPs or PMMA-MPs. Results are shown as the average value of 5–6 biological replicates ± standard error. Different lowercase letters indicate a significant difference between control and PS-MPs-treated plants, while different uppercase letters indicate a significant difference between control and PMMA-MPs-treated plants (one-way ANOVA, followed by post hoc LSD test, $p \leq 0.05$). Asterisks indicate a significant difference between two different MPs types at the same concentration (Student's *t*-test, $p \leq 0.05$).

MP type	MP concentration	F_V/F_M	PI_{ABS}	Chl *a*	Chl *b*	Cars
	(mg L^{-1})			(μg mg_{FW}^{-1})	(μg mg_{FW}^{-1})	(μg mg_{FW}^{-1})
control	0	$0.764 \pm 0.003^{b,A}$	$1.793 \pm 0.181^{b,B}$	$0.548 \pm 0.051^{bc,A}$	$0.155 \pm 0.018^{b,A}$	$0.150 \pm 0.014^{b,A}$
PS	10	$0.775 \pm 0.001^{a*}$	$2.298 \pm 0.077^{a*}$	$0.662 \pm 0.033^{ab*}$	$0.166 \pm 0.011^{ab*}$	0.187 ± 0.006^{a}
	50	0.771 ± 0.003^{ab}	$2.338 \pm 0.042^{a*}$	$0.709 \pm 0.044^{a*}$	$0.201 \pm 0.017^{a*}$	$0.201 \pm 0.010^{a*}$
	100	0.769 ± 0.005^{ab}	2.145 ± 0.157^{ab}	0.437 ± 0.056^{c}	0.132 ± 0.009^{b}	$0.127 \pm 0.013^{b*}$
PMMA	10	0.761 ± 0.003^{A}	1.892 ± 0.036^{AB}	0.416 ± 0.023^{A}	0.120 ± 0.003^{A}	0.173 ± 0.003^{A}
	50	0.763 ± 0.003^{A}	2.170 ± 0.049^{A}	0.452 ± 0.057^{A}	0.125 ± 0.014^{A}	0.163 ± 0.013^{A}
	100	0.766 ± 0.004^{A}	1.992 ± 0.090^{AB}	0.525 ± 0.044^{A}	0.13 ± 0.008^{A}	0.171 ± 0.008^{A}

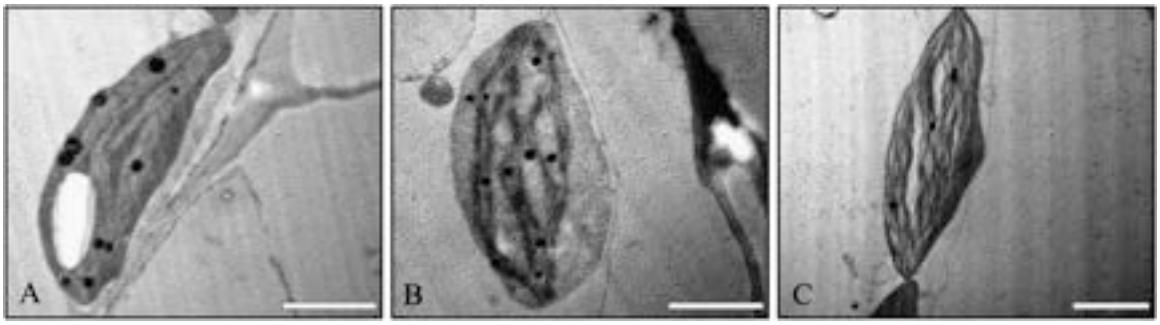

Fig. 2. Chloroplast ultrastructure in cells of *L. minor* control plants (A) and plants grown for 7 days in Steinberg nutrient medium supplemented with 100 mg L^{-1} concentration of either PS-MPs (B) or PMMA-MPs (C) imaged with transmission electron microscope. Control plants were grown in medium without MPs. Scale bar = 2 μm.

3.5. Chloroplast ultrastructure

In the control, chloroplasts with a regular thylakoid structure, numerous plastoglobules and 1–3 starch grains per organelle were observed (Fig. 2A). The measured surface area of most chloroplasts was about 12 μm^2.

After treatment with 100 mg L^{-1} PS-MPs, a greater number of round chloroplasts with a loose thylakoid system was observed, although the thylakoid membranes had a regular structure and contained stroma and grana thylakoids. These chloroplasts generally contained no starch, while the number of plastoglobules was the same or slightly higher than in the control. A lower number of chloroplasts similar to the control was also observed (Fig. 2B). The surface area of the chloroplasts was slightly larger than the control and was approximately 15 μm^2.

Exposure to 100 mg L^{-1} PMMA-MPs resulted in a higher number of chloroplasts with dilated thylakoids, most of which did not contain starch granules and had a lower number of plastoglobules than in the control and PS-MPs treatment. Holes between the thylakoid membranes were observed in these chloroplasts. However, a lower number of chloroplasts, which were similar to both controls and those after PS-MPs treatment, was also observed (Fig. 2C). The surface area of chloroplasts was similar to that after exposure to PS-MPs and was approximately 15 μm^2.

3.6. H_2O_2 content and oxidative damage of lipids and proteins

All PS-MP treatments had a large positive effect ($\eta^2 = 0.16$) on H_2O_2 content compared to the control. Moreover, the increase at 10 mg L^{-1} was statistically significant ($p \leq 0.05$). A large positive effect ($\eta^2 = 0.14$) was observed for exposure to PMMA-MPs, with a statistically significant

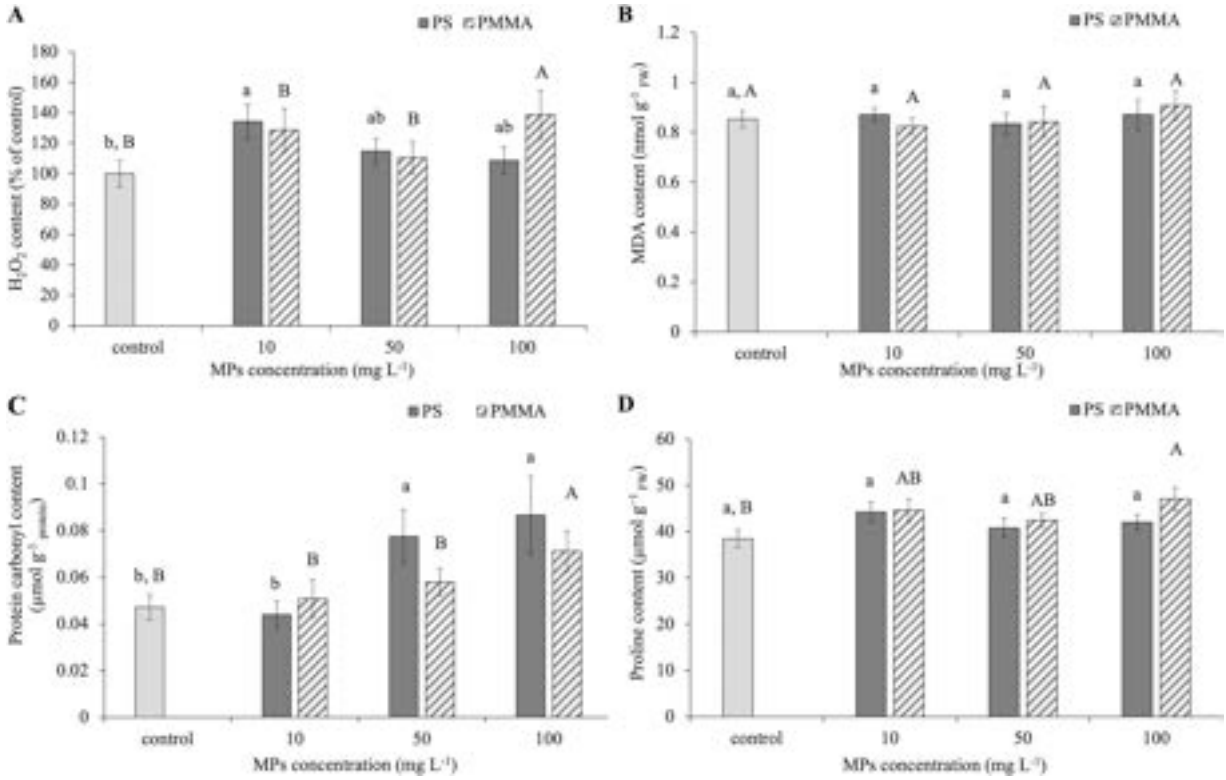

Fig. 3. Content of hydrogen peroxide (H_2O_2) (A), malondialdehyde (MDA) (B), protein carbonyls (C), and proline (D) of *L. minor* plants grown for 7 days in Steinberg nutrient medium supplemented with PS-MPs or PMMA-MPs in concentrations 10, 50, or 100 mg L^{-1}. Control plants were grown in medium without PS-MPs or PMMA-MPs. Results are shown as the average value of 10 biological replicates ± standard error. Different lowercase letters indicate a significant difference between control and PS-MP-treated plants, while different uppercase letters indicate a significant difference between control and PMMA-MP-treated plants (one-way ANOVA, followed by post hoc LSD test, $p \leq 0.05$).

($p \leq 0.05$) increase at 100 mg L^{-1}. When comparing the two MP types, a large effect was observed at 100 mg L^{-1}, with plants exposed to PMMA-MPs having 28 % higher H_2O_2 content than plants exposed to the same concentration of PS-MPs (Fig. 3A).

A positive effect of PS-MPs and PMMA-MPs on MDA content was medium ($\eta^2 = 0.10$) and low ($\eta^2 = 0.05$), respectively. Accordingly, no statistically significant changes in MDA content were recorded in any of the MP treatments tested compared to the control. MDA levles were slightly higher at 50 and 100 mg L^{-1} PMMA-MPs than at the same concentrations of PS-MPs treatment (Fig. 3B), but the effect size was small ($d < 0.5$).

On the other hand, a large effect of PS-MPs ($\eta^2 = 0.33$) and PMMA-MPs ($\eta^2 = 0.17$) on protein carbonyl content was found. Exposure to two higher concentrations of PS-MPs and the highest concentration of PMMA-MPs resulted in a statistically significant increase ($p \leq 0.05$) in protein carbonyl content compared to the control group. In addition, a large effect ($d > 0.8$) was observed when comparing PS-MPs with PMMA-MPs at 50 mg L^{-1}, and the plants treated with PS-MPs had a 35 % higher protein carbonyl content than those treated with PMMA-MPs (Fig. 3C).

3.7. Non-enzymatic and enzymatic antioxidants

The effect of PS-MPs on proline content was medium ($\eta^2 = 0.09$) and all treatments caused a slight increase in proline content compared to the control. In contrast, treatments with PMMA-MPs had a large positive effect ($\eta^2 = 0.18$), resulting in increased values compared to the control, with a statistically significant ($p \leq 0.05$) increase at 100 mg L^{-1}. A comparison between two types of treatments showed a greater effect ($d = 0.8$) for PMMA-MPs than for PS-MPs only at 100 mg L^{-1} (Fig. 3D).

Treatments with PS-MPs had no major effect ($\eta^2 = 0.03$) on SOD activity compared to the control, although a slight increase was observed at a concentration of 100 mg L^{-1}. The effect of PMMA-MPs on SOD activity was also small ($\eta^2 = 0.03$), with all treatments resulting in a slight increase in SOD activity compared to the control. Accordingly, the differences between the treatments with PS-MPs and PMMA-MPs were also small ($d \leq 0.5$) (Fig. 4A).

PS-MPs had a medium effect ($\eta^2 = 0.13$) on CAT activity. Compared to the control, 10 and 100 mg L^{-1} PS-MPs showed a slight increase in CAT activity, while a slight decrease was observed at 50 mg L^{-1}. The values obtained after exposure to 10 mg L^{-1} PS-MPs were significantly ($p \leq 0.05$) higher than those obtained at 50 mg L^{-1}. PMMA-MPs had a small effect ($\eta^2 = 0.03$) on CAT activity. Accordingly, the activity after exposure to PMMA-MPs was similar to that of the control, except at 10 mg L^{-1}, where a slight decrease was observed (Fig. 4B). Plants treated with PS-MPs showed a greater difference in effect ($d = 0.98$) with a 21 % higher CAT activity at 10 mg L^{-1} than those treated with PMMA-MPs.

Treatments with PS-MPs strongly ($\eta^2 = 0.19$) induced PPX activity. A dose-dependent increase in PPX activity, i.e. 7 %, 21 % and 30 %, was observed upon exposure to PS-MPs, and at 100 mg L^{-1} the change was statistically significant ($p \leq 0.05$) compared to the control. In contrast, PMMA-MPs had a small effect ($\eta^2 = 0.03$) on PPX activity and only caused a slight increase at the highest concentration tested. Treatments with PS-MPs mostly had large effects ($d > 0.8$), resulting in higher PPX activity compared to PMMA-MPs, which was statistically significant at 50 mg L^{-1} ($p \leq 0.05$) (Fig. 4C).

Treatments with PS-MPs had a medium inducing effect ($\eta^2 = 0.13$) on APX activity. At two higher concentrations of PS-MP treatments, a significant increase in APX activity was observed compared to the

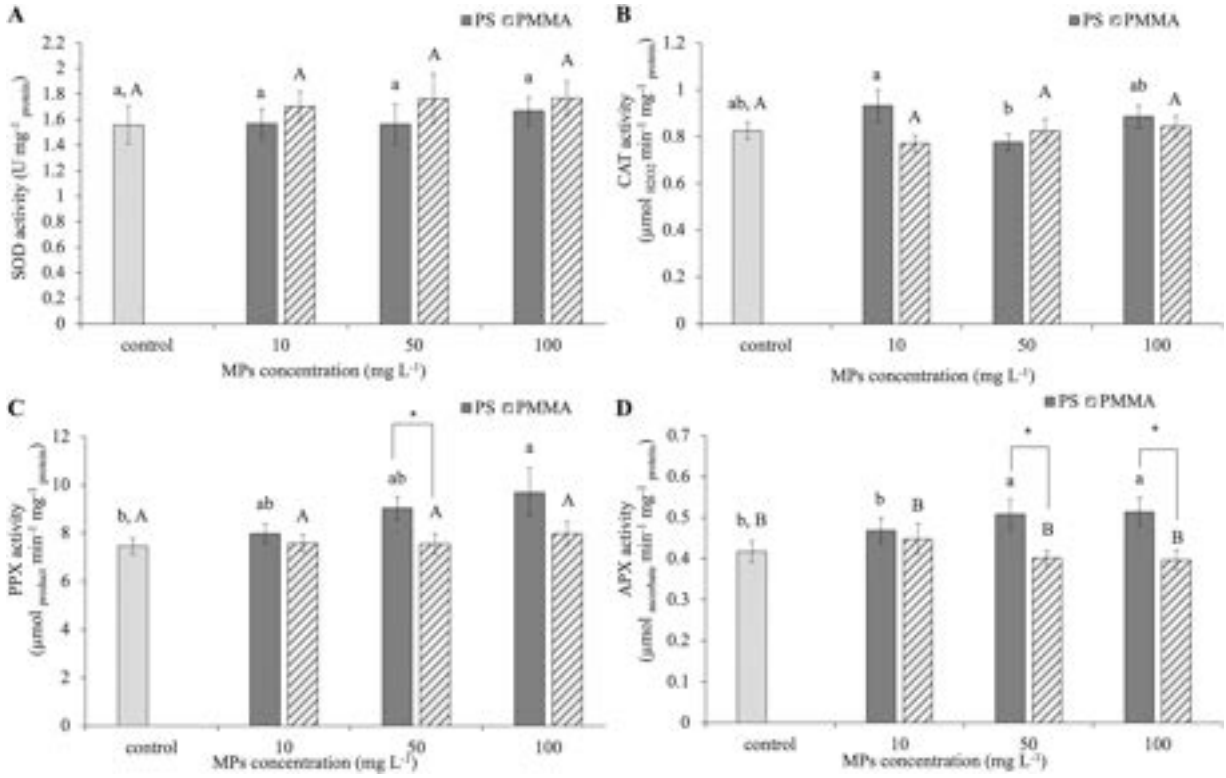

Fig. 4. Activities of antioxidative enzymes superoxide dismutase (SOD) (A), catalase (CAT) (B) pyrogallol peroxidase (PPX) (C), and ascorbate peroxidase (APX) (D) of *L. minor* plants grown for 7 days in Steinberg nutrient medium supplemented with PS-MPs or PMMA-MPs in concentrations 10, 50, or 100 mg L^{-1}. Control plants were grown in medium without PS-MPs or PMMA-MPs. Results are shown as the average value of 10 biological replicates ± standard error. Different lowercase letters indicate a significant difference between control and PS-MP-treated plants, while different uppercase letters indicate a significant difference between control and PMMA-MP-treated plants (one-way ANOVA, followed by post hoc LSD test, $p \leq 0.05$). Asterisks indicate a significant difference between two different MP types at the same concentration (Student's *t*-test, $p \leq 0.05$).

control. In contrast, PMMA-MPs had only a small effect ($\eta^2 = 0.05$), with no significant differences in APX activity observed compared to the control. When comparing two types of MPs, APX activity was significantly higher ($p \leq 0.05$) in plants exposed to 50 and 100 mg L^{-1} PS-MPs compared to the same concentrations of PMMA-MPs (Fig. 4D).

4. Discussion

The increasing presence of MPs in the aquatic environment has led to considerable concern about their potential impact on aquatic plant species such as *L. minor*. The aim of this study was to investigate the effects of MPs based on two different polymers, PS and PMMA, on *L. minor*, focusing on growth, photosynthetic performance, and oxidative stress.

4.1. Stability and uptake of PS-MPs and PMMA-MPs

Considering that the bioavailability of MPs is highly dependent on the interactions with their environment, it was important to determine the stability, i.e. the temporal changes in size and charge of MPs in the Steinberg nutrient medium prior to plant exposure. It is already known that MPs form a colloidal system in liquid medium and that their behavior is strongly influenced by the surface properties, particle size, pH, ionic strength, and temperature of the solvent [78]. In this study, signs of agglomeration were observed for both types of MPs when interacting with the culture medium. Namely, PS-MPs showed a gradual increase in d_H values only at a concentration of 10 mg L^{-1} until the fourth day, followed by dispersion of the particles on the seventh day, as evidenced by a rapid decrease in d_H values. On the contrary, PMMA-MPs showed the strongest agglomeration at the highest concentration tested. This is consistent with data from ζ-potential measurements of 100 mg L^{-1} dispersions, where negative values were measured for PS-MPs at all time points, while PMMA-MPs lost their negative charge on the seventh day and became almost neutral. It is known that colloidal particles in water acquire a surface charge that depends on the polarity, pH and salinity of the solvent [78].The higher the surface charge, the stronger the electrostatic repulsion between them and the more stable they are [79]. Although high stability of PS-MPs and PMMA-MPs in ultrapure water was reported [20,80], media with high ionic strength such as seawater and Murashige and Skoog medium promoted the agglomeration of PS particles [80,81], which is similar to our results.

The uptake and accumulation of PS-MPs and PMMA-MPs in *L. minor* tissue was confirmed by Py-GC-MS. Previously, the uptake of PS-MPs was detected by Py-GC-MS in wheat and Arabidopsis [82] and in the green alga *Chlorella sorokiniana* [83], while Li et al. [84] and Biba et al. [20] quantified PS-MPs and PMMA-MPs in cucumber plants and *Allium cepa* roots, respectively. The uptake of PMMA-MPs was also detected in *Hordeum vulgare* plants [85]. Dong et al. [86] reported that PS-MPs with a size of 1 μm accumulate in the intercellular layer of carrot roots but cannot penetrate the cells, while migration into the leaves was confirmed for PS-MPs with a size of 0.2 μm. However, uptake of nanoplastics (NPs) and MPs by leaves and translocation into roots has also been noted, and it has been suggested that the cuticle and stomatal opening may be one of the routes by which PS-NPs enter the vascular system [87,88]. Both proposed entry routes are possible in our experimental setup, as both fronds and roots of *L. minor* were directly immersed in the MPs-containing medium. Moreover, our results showed a dose-dependent increase in styrene content in the fronds of *L. minor* after 7 days of exposure to PS-MPs. Interestingly, a low styrene content was also measured in control fronds, which is consistent with the results of our previous study on *A. cepa* roots [20] and studies by other authors [82,89,90]. It can be formed from naturally occurring plant compounds with styrene-like structures by biodegradation [91] or by decarboxylation of cinnamic acid [92]. The accumulation of PMMA-MPs was less pronounced than that of PS-MPs at the same treatment concentration, which is probably due to the stronger agglomeration of PMMA-MPs. In addition, the naturally occurring styrene could explain a higher content of PS-MPs compared to PMMA-MPs at the same treatment concentration. A higher uptake of PS-MPs compared to PMMA-MPs at the same treatment concentration was also observed in onion [20] and cucumber roots [93].

4.2. Growth and photosynthesis

Previous research has frequently documented the detrimental effects of MPs on plant growth and physiology, with the usual consequences of reduced growth rates and impaired photosynthesis. Xiao et al. [94] showed growth inhibition in *L. minor* exposed to PS-MPs at concentrations of up to 50 mg L^{-1}. Similarly, fluorescent PS-MPs were shown to negatively affect the growth of another aquatic plant, *Utricularia vulgaris* L., but at higher concentrations [95]. However, the effects of MPs on aquatic plants were not always clear, but depended on the size, type, and concentration of MPs. For example, Mateos-Cárdenas et al. [59] found no significant effects of 10–45 μm PE microspheres on *L. minor*, while Kalčíková et al. [55] observed only minor effects of 71 μm PE fragments. On the other hand, Rozman et al. [6,61] emphasized the harmful effects of larger MPs, such as 149 μm PE fragments and 47 μm tire wear particles, mainly due to mechanical abrasion by particles with sharp edges. Our results showed a more differentiated response of *L. minor* to MPs, with PS-MPs and PMMA-MPs triggering different physiological effects. While PS-MPs at lower concentrations (10 and 50 mg L^{-1}) seemed to have a strong positive effect on growth, especially on frond area and photosynthetic performance, PMMA-MPs showed pronounced negative effects, especially at the highest concentration (100 mg L^{-1}). This difference in responses is probably due to the specific physico-chemical properties of MPs, which may influence the ecotoxicity of MPs [61]. As noted in several studies [96,97], agglomeration of MPs can impair or block nutrient uptake by adhering to the roots, which could disrupt water transport within the plant and physically damage plant tissue. Analysis of MPs stability revealed agglomeration of PMMA-MPs in the culture medium, which may have negatively affected the growth of *L. minor* by limiting the availability of dissolved nutrients. This is confirmed by the photosynthetic pigment results as discussed below.

As far as photosynthesis is concerned, the results are in close agreement with the observed growth patterns. Both F_V/F_M and PI_{ABS} as well as the content of photosynthetic pigments (chlorophyll *a*, chlorophyll *b* and carotenoids) were higher in plants exposed to 10 and 50 mg L^{-1} PS-MPs than to the corresponding concentrations of PMMA-MPs. The improved photosynthetic efficiency and increased pigment content may explain the growth stimulation observed in PS-MP-treated plants. Lian et al. [98] found that PS-NPs promoted the growth of wheat seedlings by improving photosynthetic gas exchange parameters and Chl *a* content. Moreover, PS-NPs stimulated the carbon assimilation rate at a low dose but decreased it at a high dose [99] The increased pigment content observed in our study could be the result of altered light availability, as microplastic particles can affect the initial transmission of light radiation in water bodies [100]. This is also supported by the results of the JIP-test, which showed a decrease in energy absorbed, captured and dissipated per reaction center, but an increase in RC/CS_o, especially after treatments with PS-MPs. Such responses are characteristic of *L. minor* plants adapted to low-light conditions [101] and could be related to the increase in frond surface area capable of photosynthesis observed in our study. In addition, the increase in carotenoid content not only supports photosynthesis but also has an antioxidant effect that likely helps to mitigate oxidative damage and supports both photosynthetic activity and overall plant health under PS-MPs exposure. In contrast, the impaired pigment biosynthesis and reduced photosynthetic efficiency in PMMA-MP-treated plants could be the result of reduced nutrient availability due to PMMA-MPs agglomeration. In support of this hypothesis, Ozfidan-Konakci et al. [102] reported a greater reduction in nitrogen content in *L. minor* when exposed to PMMA-MPs than when exposed to PS-MPs, emphasizing the greater nutrient deprivation by

PMMA-MPs. Chlorophyll biosynthesis is highly dependent on essential nutrients such as nitrogen, magnesium, and iron [103,104]. The reduction in chlorophyll content would directly affect photosynthetic capacity, as chlorophyll plays a central role in light absorption and energy conversion during photosynthesis [105]. As a result, lower chlorophyll content would reduce the plant's ability to capture light and sustain photosynthetic reactions, ultimately leading to lower photosynthetic efficiency (e.g. lower F_V/F_M and PI_{ABS} levels) and inhibited growth, as observed in PMMA-treated plants. Interestingly, at the highest concentration of PS-MPs (100 mg L^{-1}), photosynthetic efficiency and growth of *L. minor* were not impaired despite the observed lower amount of photosynthetic pigments. Our analysis of chloroplast ultrastructure supports these results, as 100 mg L^{-1} PS-MPs caused only moderate structural changes such as a looser thylakoid arrangement and a slight increase in chloroplast size. However, the integrity of the thylakoid membrane remained largely intact, suggesting that the reduction in pigment content was not the result of damage to the photosynthetic machinery but rather an adaptive response. In contrast, PMMA-MPs caused more severe ultrastructural changes in chloroplasts, including thylakoid dilatation, fewer plastoglobules, and the formation of gaps between thylakoid membranes. These more pronounced disruptions in chloroplast structure associated with reduced pigment content could be the result of increased H_2O_2 levels observed in the plants treated with 100 mg L^{-1} PMMA-MPs, which likely contributed to the inhibited growth. The severe impairment of photosynthesis in the plants treated with PMMA-MPs was further confirmed by substantial decrease in rbcL, the primary carboxylase of the photosynthetic process. So far, several authors have reported down-regulated expression of genes or proteins involved in photosynthesis as a possible molecular mechanism for the toxicity of MPs. In *Nicotiana tabacum* seedlings, a 48-day exposure to PE-MPs resulted in a significant increase in superoxide anion content, a decrease in chlorophyll content and RuBisCO activity, as well as the down-regulation of genes involved in light harvesting, electron transport and photosystem-related processes [106]. In the freshwater microalga *Chlamydomonas reinhardtii*, exposure to PS-MPs and PVC-MPs inhibited growth and induced stronger oxidative stress than PP-MPs and PE-MPs, which was correlated with a prominent reduction in the expression of photosynthetic proteins [107]. In addition, smaller PS-MNPs were shown to reduce chlorophyll content and F_V/F_M more significantly than larger ones, which is due to suppressed expression of photosynthesis-related proteins, especially those involved in light harvesting [108].

4.3. Oxidative stress and damage to important biomolecules

The imbalance in the generation and neutralization of reactive oxygen species (ROS) leads to oxidative stress, which is considered to be one of the mechanisms of phytotoxicity of MPs [109]. An excess of ROS in the cells can damage important biomolecules, i.e. proteins and nucleic acids, and impair physiological and metabolic processes [110].

In this study, all treatments caused a slight increase in H_2O_2, a non-radical ROS, while causing no prominent damage to lipids, as evidenced by no significant changes in MDA content. The highest increase in H_2O_2 content was observed at 100 mg L^{-1} PMMA-MPs, which can be associated with the largest observed decrease in growth rate among the tested treatments. Indeed, it has been reported that increased H_2O_2 concentrations can trigger an oxidative burst and impair plant growth [111,112]. Moreover, protein carbonyl content was increased at two higher concentrations of both types of MPs in our study. Similar to our results, the MDA content did not change in *A. cepa* roots exposed to 10, 100 and 1000 mg L^{-1} PS-MPs and PMMA-MPs for 3 days, while the H_2O_2 content increased at the highest PS-MPs concentration [20]. However, the same treatments had no effect on protein carbonyl content [20], which is in contradiction with our results. In contrast, increased MDA content was observed in another aquatic plant, *Salvinia cucullata* [113] and in cucumber roots [93] treated with PS-MPs of 1 μm and 300 nm in size, respectively, as well as in *Allium sativum* leaves treated with 0.5 and 1 mg g^{-1} PS-NPs with an average size of 75 nm [114]. In *A. cepa* roots, Maity et al. [115] found a significantly increased MDA content after exposure to PS-MPs of 100 nm (100–400 mg L^{-1}), while Giorgetti et al. [40] observed an increased H_2O_2 and MDA content after exposure to 50 nm PS-MPs of 0.01–1 g L^{-1}. The study by Li et al. [116] showed that the size of MPs was the most important determinant of phytotoxicity, where at the same concentration of PS-MPs treatment (50 mg L^{-1}) with four different particle sizes (100, 300, 500 and 700 nm), only the 700 nm PS-MPs caused an increase in H_2O_2 and MDA levels in cucumber leaves compared to the control. The inconsistency of the results presented suggests that several factors play a role in the response of plants to MPs/NPs treatment, including plant species, organ type, particle size and stability in different exposure media, treatment concentration as well as exposure method and chemical properties of the different polymers [117].

4.4. Activation of non-enzymatic and enzymatic antioxidant defense

To maintain redox homeostasis in cells and preserve the integrity of biomolecules, plants activate a system of enzymatic and non-enzymatic antioxidants [118]. In our study, we measured the content of proline, an amino acid that is considered a non-enzymatic antioxidant due to its ability to neutralize various ROS, especially singlet oxygen ($^1O_2$) and H_2O_2 [119], while inhibiting the process of lipid peroxidation to maintain the integrity of cell membranes [120]. Proline content increased slightly in all treatments, but significantly only in the treatment with 100 mg L^{-1} PMMA-MPs, which is consistent with the observations of Ozfidan-Konakci et al. [102] for *L. minor* treated with PS-NPs and PMMA-NPs. In contrast, proline content was reduced in cucumber leaves after treatment with 100 nm PS-NPs [116], but increased in leaves treated with 700 nm PS-NPs [116] and in roots exposed to 300 nm PS-NPs [93], suggesting that the specific responses depend on the particular properties of the MPs/NPs and vary between species.

One of the most effective antioxidants and the first line of defense against ROS is the enzyme SOD, which catalyzes the conversion of $O_2^{\bullet-}$ to H_2O_2, which is then degraded by the enzymes CAT and peroxidases [121]. Our results showed a slight increase in SOD activity after treatments with PMMA-MPs, while the activities of PPX and APX both increased after exposure to PS-MPs, especially at higher concentrations, which could be related to the lower H_2O_2 content in these plants. In addition, no clear difference in CAT activity was observed in any of the treatments tested. Considering that the treatment duration in our study was 7 days, this could be explained by the different reactivity of the antioxidant enzymes, with CAT showing increased activity in the early stress phases and the peroxidases responding in later phases [122]. To test this hypothesis, further studies should include measurements at multiple time points during the exposure period, as this could provide a more comprehensive understanding of the temporal patterns of stress responses. There are two possible explanations for the different effects of the two types of MP tested in our study on antioxidant enzymes: (i) the type of polymer has an effect on the activation of specific components of the antioxidant defense, as evidenced by a slight increase in SOD activities at all PMMA-MP concentrations tested, in contrast to an increase in peroxidase activity in PS-MP-treated plants; (ii) the bioavailability of the two polymers in the exposure medium was different due to their different chemical properties. Although the PMMA-MPs were initially smaller, they agglomerated more readily in the Steinberg nutrient medium than the PS-MPs, so that their uptake was more impeded and therefore no antioxidant response was induced. On the other hand, PS-MPs, being more stable, penetrated more easily into the plants, as confirmed by the accumulation analysis, and triggered more oxidative stress symptoms. In general, higher concentrations of MPs/NPs decrease the activities of antioxidant enzymes, while lower concentrations may initially increase them, although concentration, size, and surface properties may influence these effects [121]. Up-regulation of genes

encoding antioxidant enzymes in response to MP-induced oxidative stress has been reported [123]. In another aquatic plant, *Salvinia cucullata*, an increase in the activities of SOD, APX and CAT was observed after exposure to similar concentrations of PS-MPs and exposure time as in our experiment [113]. However, the particle size in this study was much larger than in ours (1 μm), which together with the differences in plant species could explain the difference in antioxidant response. In addition, a decrease in CAT activity was observed in *Vicia faba* roots after treatment with 5 μm-sized PS-MPs at 100 mg L^{-1}, whereas when 100 nm-sized particles were applied, the activities of SOD, PPX and CAT increased [39]. An increase in SOD, CAT and POD activities was also observed in rice roots after treatment with 10–100 mg L^{-1} PS-MPs with a particle size of 20 nm [124]. Biba et al. [20] reported activation of enzymatic antioxidants in onion roots treated with PS-MPs and PMMA-MPs, especially CAT and PPX. In contrast, a reduction in the activities of SOD, POD and CAT was observed in rice grown from seeds in a medium containing 1 g L^{-1} PS-MPs with a size of 200 nm [125], suggesting that different plant species show a different antioxidant response to the toxicity of MPs. This response depends on a number of factors in which the size of the particles and the concentration of the treatment play a crucial role.

4.5. Environmental relevance of the investigated MPs

Despite the unfavorable effects observed in this study on some of the parameters tested, neither type of MPs was found to have a serious toxic effect on *L. minor* plants, which could be at least partially attributed to their properties. We used commercially available spherical MPs produced with high purity and uniform size and without any additives. Studies show that spherical MPs generally have lower toxicity and uptake by aquatic organisms than irregularly shaped particles because their smooth shape minimizes interaction with biological tissue [126, 127]. Irregular MPs, such as fragments and fibers, which are commonly found in the environment, are more toxic because they adsorb chemicals more strongly and have higher bioaccumulation, as well as due to their rough surface, which enhances physical interactions with biological membranes and causes greater damage [128,129]. As previously mentioned, studies on aquatic plants have shown that MPs shape has no effect on growth rate or chlorophyll content, but fragments and films have higher adsorption capacity and reduce root growth compared to spherical MPs [57,61].

Moreover, we used MPs made of pure polymers, which generally do not have strong negative effects on plants [61,130]. The presence of additives in MPs such as plasticizers, flame retardants and antioxidants [131] or adsorbed environmental chemicals [132] plays an important role in their ecotoxicity to aquatic organisms. These chemicals can be more toxic than the MPs themselves by interfering with plant growth and physiology, causing oxidative stress and reducing photosynthesis and photosynthetic pigments [6,133]. PS and PMMA differ in their leaching properties due to their chemical composition and structure. PS, a hydrophobic polymer, releases more additives such as plasticizers and stabilizers, while PMMA, which has a stiffer and more hydrophilic structure, leaches fewer additives [134], but can release residual monomers such as MMA under certain conditions [135]. Namely, plastics contain monomers and oligomers that originate from the production process through incomplete polymerization. The possibility of leaching of monomers, short-chain polymers and a range of chemical additives shows that the chemical identity of plastics in the environment is an extremely complex issue that is only just beginning to be addressed [136].

5. Conclusion

The comparison between PS-MPs and PMMA-MPs shows different effects on the growth and physiological processes of *L. minor*. PS-MPs are smaller and less prone to agglomeration, so that they can be more easily taken up by the plants. This leads to a mild oxidative stress, which activates peroxidases such as PPX and APX. They also increase the content of photosynthetic pigments and increase photosynthetic efficiency, which is associated with stimulated growth. In contrast, PMMA-MPs exhibit lower uptake and greater agglomeration and have a more detrimental effect on *L. minor*. They reduce growth, photosynthetic efficiency and pigment content while causing severe ultrastructural damage in the chloroplasts. Interestingly, PMMA-MPs do not induce pronounced oxidative damage, suggesting a different mechanism of toxicity compared to PS-MPs.

Funding sources

This work was supported by the Croatian Science Foundation under the project number [HRZZ- IP-2022–10–3824], and European Regional Development Fund (infrastructural project CIuK, grant number KK.01.1.1.02.0016).

Authors statement

All authors have approved the paper and agree with all changes made in the paper.

Declaration of Competing Interest

The authors declare that they have no known competing financial interests or personal relationships that could have appeared to influence the work reported in this paper.

Appendix A. Supporting information

Supplementary data associated with this article can be found in the online version at doi:10.1016/j.cpb.2025.100473.

Data availability

Data will be made available on request.

References

[1] P.G.C. Nayanathara Thathsarani Pilapitiya, A.S. Ratnayake, The world of plastic waste: a review, Clean. Mater. 11 (2024), https://doi.org/10.1016/j.clema.2024.100220.
[2] S. Gabbott, S. Key, C. Russell, Y. Yonan, J. Zalasiewicz, The geography and geology of plastics: their environmental distribution and fate. in: Plastic Waste and Recycling: Environmental Impact, Societal Issues, Prevention, and Solutions, Elsevier, 2020, pp. 33–63, https://doi.org/10.1016/B978-0-12-817880-5.00003-7.
[3] R. Hurley, A. Horton, A. Lusher, L. Nizzetto, Plastic waste in the terrestrial environment. in: Plastic Waste and Recycling: Environmental Impact, Societal Issues, Prevention, and Solutions, Elsevier, 2020, pp. 163–193, https://doi.org/10.1016/B978-0-12-817880-5.00007-4.
[4] V.M. Azevedo-Santos, M.F.G. Brito, P.S. Manoel, J.F. Perroca, J.L. Rodrigues-Filho, L.R.P. Paschoal, G.R.L. Gonçalves, M.R. Wolf, M.C.M. Blettler, M. C. Andrade, A.B. Nobile, F.P. Lima, A.M.C. Ruocco, C.V. Silva, G. Perbiche-Neves, J.L. Portinho, T. Giarrizzo, M.S. Arcifa, F.M. Pelicice, Plastic pollution: a focus on freshwater biodiversity, Ambio 50 (2021) 1313–1324, https://doi.org/10.1007/s13280-020-01496-5.
[5] B.A. Walther, M. Bergmann, Plastic pollution of four understudied marine ecosystems: a review of mangroves, seagrass meadows, the Arctic Ocean and the deep seafloor, Emerg. Top. Life Sci. 6 (2022) 371–387, https://doi.org/10.1042/ETLS20220017.
[6] U. Rozman, G. Kalčíková, The response of duckweed *Lemna minor* to microplastics and its potential use as a bioindicator of microplastic pollution, Plants 11 (2022) 2953–2964, https://doi.org/10.3390/plants11212953.
[7] P. Farrell, K. Nelson, Trophic level transfer of microplastic: *Mytilus edulis* (L.) to *Carcinus maenas* (L.), Environ. Pollut. 177 (2013) 1–3, https://doi.org/10.1016/j.envpol.2013.01.046.
[8] F. Gallo, C. Fossi, R. Weber, D. Santillo, J. Sousa, I. Ingram, A. Nadal, D. Romano, Marine litter plastics and microplastics and their toxic chemicals components: the need for urgent preventive measures, Environ. Sci. Eur. 30 (2018) 13–27, https://doi.org/10.1186/s12302-018-0139-z.

[9] I.A. Kane, M.A. Clare, Dispersion, accumulation, and the ultimate fate of microplastics in deep-marine environments: a review and future directions, Front. Earth Sci. 7 (2019) 80–107, https://doi.org/10.3389/feart.2019.00080.
[10] I.A. Kane, M.A. Clare, E. Miramontes, R. Wogelius, J.J. Rothwell, P. Garreau, F. Pohl, Seafloor microplastic hotspots controlle by deep-sea circulation, Science (1979) 368 (2020) 1140–1145, https://doi.org/10.1126/science.aba5899.
[11] J. John, A.R. Nandhini, P. Velayudhaperumal Chellam, M. Sillanpää, Microplastics in mangroves and coral reef ecosystems: a review, Environ. Chem. Lett. 20 (2022) 397–416, https://doi.org/10.1007/s10311-021-01326-4.
[12] M. Sajjad, Q. Huang, S. Khan, M.A. Khan, Y. Liu, J. Wang, F. Lian, Q. Wang, G. Guo, Microplastics in the soil environment: a critical review, Environ. Technol. Innov. 27 (2022) 102408–102433, https://doi.org/10.1016/j.eti.2022.102408.
[13] P.D. Dissanayake, S. Kim, B. Sarkar, P. Oleszczuk, M.K. Sang, M.N. Haque, J. H. Ahn, M.S. Bank, Y.S. Ok, Effects of microplastics on the terrestrial environment: a critical review, Environ. Res. 209 (2022), https://doi.org/10.1016/j.envres.2022.112734.
[14] L.D. Yardy, R. Al-Jaibachi, A. Callaghan, Microplastics in freshwater ecosystems with special reference to tropical systems: Detection, impact, and management. in: Emerging Freshwater Pollutants, Elsevier, 2022, pp. 151–169, https://doi.org/10.1016/B978-0-12-822850-0.00017-X.
[15] L.K. Bhardwaj, P. Rath, P. Yadav, U. Gupta, Microplastic contamination, an emerging threat to the freshwater environment: a systematic review, Environ. Syst. Res. 13 (2024) 1–17, https://doi.org/10.1186/s40068-024-00338-7.
[16] I. Gambino, F. Bagordo, T. Grassi, A. Panico, A. De Donno, Occurrence of microplastics in tap and bottled water: current knowledge, Int. J. Environ. Res. Public Health 19 (2022) 5283, https://doi.org/10.3390/ijerph19095283.
[17] C.V. Neves, C.C. Gaylarde, J.A. Baptista Neto, K.S. Vieira, B. Pierri, C.C.C. Waite, D.C. Scott, E.M. da Fonseca, The transfer and resulting negative effects of nano- and micro-plastics through the aquatic trophic web – a discreet threat to human health, Water Biol. Secur. 1 (2022) 100080, https://doi.org/10.1016/j.watbs.2022.100080.
[18] V. Hidalgo-Ruz, L. Gutow, R.C. Thompson, M. Thiel, Microplastics in the marine environment: a review of the methods used for identification and quantification, Environ. Sci. Technol. 46 (2012) 3060–3075, https://doi.org/10.1021/es2031505.
[19] R. Shi, W. Liu, Y. Lian, Q. Wang, A. Zeb, J. Tang, Phytotoxicity of polystyrene, polyethylene and polypropylene microplastics on tomato (*Lycopersicon esculentum* L.), J. Environ. Manag. 317 (2022) 115441, https://doi.org/10.1016/j.jenvman.2022.115441.
[20] R. Biba, P. Cvjetko, M. Jakopčić, B. Komazec, M. Tkalec, N. Dimitrov, T. Begović, B. Balen, Phytotoxic effects of polystyrene and polymethyl methacrylate microplastics on *Allium cepa* roots, Plants 12 (2023) 747–769, https://doi.org/10.3390/plants12040747.
[21] Y. Lian, R. Shi, J. Liu, A. Zeb, Q. Wang, J. Wang, M. Yu, J. Li, Z. Zheng, N. Ali, Y. Bao, W. Liu, Effects of polystyrene, polyethylene, and polypropylene microplastics on the soil-rhizosphere-plant system: phytotoxicity, enzyme activity, and microbial community, J. Hazard. Mater. 465 (2024) 133417, https://doi.org/10.1016/j.jhazmat.2023.133417.
[22] C.M. Rochman, E. Hoh, B.T. Hentschel, S. Kaye, Long-term field measurement of sorption of organic contaminants to five types of plastic pellets: implications for plastic marine debris, Environ. Sci. Technol. (2013) 1646–1654, https://doi.org/10.1021/es303700s.
[23] K. Duis, A. Coors, Microplastics in the aquatic and terrestrial environment: sources (with a specific focus on personal care products), fate and effects, Environ. Sci. Eur. 28 (2016) 1–25, https://doi.org/10.1186/s12302-015-0069-y.
[24] A. Rossatto, M.Z.F. Arlindo, M.S. de Morais, T.D. de Souza, C.S. Ogrodowski, Microplastics in aquatic systems: a review of occurrence, monitoring and potential environmental risks, Environ. Adv. 13 (2023) 100396, https://doi.org/10.1016/j.envadv.2023.100396.
[25] A. Bellasi, G. Binda, A. Pozzi, S. Galafassi, P. Volta, R. Bettinetti, Microplastic contamination in freshwater environments: a review, focusing on interactions with sediments and benthic organisms, Environments 7 (2020) 30–60, https://doi.org/10.3390/environments7040030.
[26] N.N. Jalaudin Basha, N.B. Adzuan Hafiz, M.S. Osman, N.F. Abu Bakar, Unveiling the noxious effect of polystyrene microplastics in aquatic ecosystems and their toxicological behavior on fishes and microalgae, Front. Toxicol. 5 (2023), https://doi.org/10.3389/ftox.2023.1135081.
[27] M. Shen, Z. Zeng, X. Wen, X. Ren, G. Zeng, Y. Zhang, R. Xiao, Presence of microplastics in drinking water from freshwater sources: the investigation in Changsha, China, Environ. Sci. Pollut. Res. 28 (2021) 42313–42324, https://doi.org/10.1007/s11356-021-13769-x.
[28] R. Gautam, A.S. Bassi, E.K. Yanful, A review of biodegradation of synthetic plastic and foams, Appl. Biochem. Biotechnol. 141 (2007) 85–108, https://doi.org/10.1007/s12010-007-9212-6.
[29] B.T. Ho, T.K. Roberts, S. Lucas, An overview on biodegradation of polystyrene and modified polystyrene: the microbial approach, Crit. Rev. Biotechnol. 38 (2018) 308–320, https://doi.org/10.1080/07388551.2017.1355293.
[30] M. Kaur, M. Xu, L. Wang, Cyto–genotoxic effect causing potential of polystyrene micro-plastics in terrestrial plants, Nanomaterials 12 (2022) 2024, https://doi.org/10.3390/nano12122024.
[31] M. Kuroda, A. Isobe, K. Uchida, T. Tokai, T. Kitakado, M. Yoshitake, Y. Miyamoto, T. Mukai, K. Imai, K. Shimizu, M. Yagi, T. Mituhasi, A. Habano, Abundance and potential sources of floating polystyrene foam macro- and microplastics around Japan, Sci. Total Environ. 925 (2024) 171421, https://doi.org/10.1016/j.scitotenv.2024.171421.
[32] S.A. Siddiqui, S. Singh, N.A. Bahmid, D.J.H. Shyu, R. Domínguez, J.M. Lorenzo, J. A.M. Pereira, J.S. Câmara, Polystyrene microplastic particles in the food chain: characteristics and toxicity – a review, Sci. Total Environ. 892 (2023) 164531, https://doi.org/10.1016/j.scitotenv.2023.164531.
[33] J. Hwang, D. Choi, S. Han, S.Y. Jung, J. Choi, J. Hong, Potential toxicity of polystyrene microplastic particles, Sci. Rep. 10 (2020), https://doi.org/10.1038/s41598-020-64464-9.
[34] J. Yan, Y. Pan, J. He, X. Pang, W. Shao, C. Wang, R. Wang, Y. He, M. Zhang, J. Ye, C. Lin, F. Lin, Y. Wang, T. Li, Y. Lan, Y. Guo, M. Wang, M. Sun, Y. Gong, M. Yuan, D. Yin, X. Sun, S. Dong, Toxic vascular effects of polystyrene microplastic exposure, Sci. Total Environ. 905 (2023) 167215, https://doi.org/10.1016/j.scitotenv.2023.167215.
[35] J. Zheng, C. Li, X. Zheng, Toxic effects of polystyrene microplastics on the intestine of *Amphioctopus fangsiao* (Mollusca: Cephalopoda): from physiological responses to underlying molecular mechanisms, Chemosphere 308 (2022) 136362, https://doi.org/10.1016/j.chemosphere.2022.136362.
[36] A. Saeed, M.F. Akhtar, A. Saleem, B. Akhtar, A. Sharif, Reproductive and metabolic toxic effects of polystyrene microplastics in adult female Wistar rats: a mechanistic study, Environ. Sci. Pollut. Res. 30 (2023) 63185–63199, https://doi.org/10.1007/s11356-023-26565-6.
[37] S. Li, P. Wang, C. Zhang, X. Zhou, Z. Yin, T. Hu, D. Hu, C. Liu, L. Zhu, Influence of polystyrene microplastics on the growth, photosynthetic efficiency and aggregation of freshwater microalgae *Chlamydomonas reinhardtii*, Sci. Total Environ. 714 (2020), https://doi.org/10.1016/j.scitotenv.2020.136767.
[38] D. Wu, T. Wang, J. Wang, L. Jiang, Y. Yin, H. Guo, Size-dependent toxic effects of polystyrene microplastic exposure on *Microcystis aeruginosa* growth and microcystin production, Sci. Total Environ. 761 (2021) 143265, https://doi.org/10.1016/j.scitotenv.2020.143265.
[39] X. Jiang, H. Chen, Y. Liao, Z. Ye, M. Li, G. Klobučar, Ecotoxicity and genotoxicity of polystyrene microplastics on higher plant *Vicia faba*, Environ. Pollut. 250 (2019) 831–838, https://doi.org/10.1016/j.envpol.2019.04.055.
[40] L. Giorgetti, C. Spanò, S. Muccifora, S. Bottega, F. Barbieri, L. Bellani, M. Ruffini Castiglione, Exploring the interaction between polystyrene nanoplastics and *Allium cepa* during germination: internalization in root cells, induction of toxicity and oxidative stress, Plant. Physiol. Biochem 149 (2020) 170–177, https://doi.org/10.1016/j.plaphy.2020.02.014.
[41] J. De Tommaso, J.-L. Dubois, Risk analysis on PMMA recycling economics, Polym. (Basel) 13 (2021) 2724, https://doi.org/10.3390/polym13162724.
[42] M. Sivakumar, K.Panduranga Rao, Synthesis and characterization of poly(methyl methacrylate) functional microspheres, React. Funct. Polym. 46 (2000) 29–37, https://doi.org/10.1016/S1381-5148(00)00033-X.
[43] T. Gouin, J. Avalos, I. Brunning, K. Brzuska, J. de Graaf, J. Kaumanns, T. Konong, M. Meyberg, K. Rettinger, H. Schlatter, J. Thomas, R. van Welie, T. Wolf, Use of micro-plastic beads in cosmetic products in Europe and their estimated emissions to the North Sea environment, SOFW J. 141 (2015) 40–46. ⟨https://www.researchgate.net/publication/291326701⟩.
[44] E. Esmizadeh, S. Khalili, A. Vahidifar, G. Naderi, C. Dubois, Waste polymethyl methacrylate (PMMA): Recycling and high-yield monomer recovery. in: Handbook of Ecomaterials, Springer International Publishing, Cham, 2019, pp. 2977–3009, https://doi.org/10.1007/978-3-319-68255-6_164.
[45] J. Dong, L. Li, Q. Liu, M. Yang, Z. Gao, P. Qian, K. Gao, X. Deng, Interactive effects of polymethyl methacrylate (PMMA) microplastics and salinity variation on a marine diatom *Phaeodactylum tricornutum*, Chemosphere 289 (2022) 133240, https://doi.org/10.1016/j.chemosphere.2021.133240.
[46] R. Dong, R. Liu, Y. Xu, W. Liu, L. Wang, X. Liang, Q. Huang, Y. Sun, Single and joint toxicity of polymethyl methacrylate microplastics and As (V) on rapeseed (*Brassica campestris* L.), Chemosphere 291 (2022) 133066, https://doi.org/10.1016/j.chemosphere.2021.133066.
[47] D. Pavičić-Hamer, I. Kovačić, T. Sović, M. Marelja, D.M. Lyons, Exposure to polymethylmethacrylate microplastics induces a particle size-dependent immune response in mediterranean mussel *Mytilus galloprovincialis*, Fishes 7 (2022) 307, https://doi.org/10.3390/fishes7060307.
[48] P. Keddy, Plants and Vegetation, Cambridge University Press, 2007, https://doi.org/10.1017/CBO9780511812989.
[49] M.A. Urbina, F. Correa, F. Aburto, J.P. Ferrio, Adsorption of polyethylene microbeads and physiological effects on hydroponic maize, Sci. Total Environ. 741 (2020) 140216, https://doi.org/10.1016/j.scitotenv.2020.140216.
[50] S. Li, T. Wang, J. Guo, Y. Dong, Z. Wang, L. Gong, X. Li, Polystyrene microplastics disturb the redox homeostasis, carbohydrate metabolism and phytohormone regulatory network in barley, J. Hazard Mater. 415 (2021), https://doi.org/10.1016/j.jhazmat.2021.125614.
[51] L. Teng, Y. Zhu, H. Li, X. Song, L. Shi, The phytotoxicity of microplastics to the photosynthetic performance and transcriptome profiling of *Nicotiana tabacum* seedlings, Ecotoxicol. Environ. Saf. 231 (2022) 113155, https://doi.org/10.1016/j.ecoenv.2021.113155.
[52] G. Kalčíková, Aquatic vascular plants – a forgotten piece of nature in microplastic research, Environ. Pollut. 262 (2020) 114354, https://doi.org/10.1016/j.envpol.2020.114354.
[53] D.M. Osman, W. Yuan, S. Shabaka, M.P. Nyaga, J. Geng, Y. Yu, Y. Yang, The threat of micro/nanoplastic to aquatic plants: current knowledge, gaps, and future perspectives, Aquat. Toxicol. 265 (2023) 106771, https://doi.org/10.1016/j.aquatox.2023.106771.
[54] R.A. Laird, P.M. Barks, Skimming the surface: duckweed as a model system in ecology and evolution, Am. J. Bot. 105 (2018) 1962–1966, https://doi.org/10.1002/ajb2.1194.

[55] G. Kalčíková, A. Žgajnar Gotvajn, A. Kladnik, A. Jemec, Impact of polyethylene microbeads on the floating freshwater plant duckweed *Lemna minor*, Environ. Pollut. 230 (2017) 1108–1115, https://doi.org/10.1016/j.envpol.2017.07.050.
[56] D. Eerkes-Medrano, R.C. Thompson, D.C. Aldridge, Microplastics in freshwater systems: a review of the emerging threats, identification of knowledge gaps and prioritisation of research needs, Water Res. 75 (2015) 63–82, https://doi.org/10.1016/j.watres.2015.02.012.
[57] M. Miloloža, U. Rozman, D. Kučić Grgić, G. Kalčikova, Aquatic toxicity of polyethylene and microcrystalline cellulose microbeads used as abrasives in cosmetics, Chem. Biochem. Eng. Q. (2023), https://doi.org/10.15255/CABEQ.2023.2181.
[58] U. Rozman, A. Jemec Kokalj, A. Dolar, D. Drobne, G. Kalčíková, Long-term interactions between microplastics and floating macrophyte *Lemna minor*: the potential for phytoremediation of microplastics in the aquatic environment, Sci. Total Environ. 831 (2022) 154866, https://doi.org/10.1016/j.scitotenv.2022.154866.
[59] A. Mateos-Cárdenas, D.T. Scott, G. Seitmaganbetova, F.N.A.M. van Pelt, J. O'Halloran, M.A.K. Jansen, Polyethylene microplastics adhere to *Lemna minor* (L.), yet have no effects on plant growth or feeding by *Gammarus duebeni* (Lillj.), Sci. Total Environ. 689 (2019) 413–421, https://doi.org/10.1016/j.scitotenv.2019.06.359.
[60] S. Ceschin, F. Mariani, D. Di Lernia, I. Venditti, E. Pelella, M.A. Iannelli, Effects of microplastic contamination on the aquatic plant *Lemna minuta* (least duckweed), Plants 12 (2023) 207, https://doi.org/10.3390/plants12010207.
[61] U. Rozman, T. Turk, T. Skalar, M. Zupančič, N. Čelan Korošin, M. Marinšek, J. Olivero-Verbel, G. Kalčíková, An extensive characterization of various environmentally relevant microplastics – material properties, leaching and ecotoxicity testing, Sci. Total Environ. 773 (2021) 145576, https://doi.org/10.1016/j.scitotenv.2021.145576.
[62] ISO-20079-2005, Water quality – Determination of the toxic effect of water constituents and waste water to duckweed (*Lemna minor*) - Duckweed Growth Inhibition Test., Geneva, 2005.
[63] A. Pirson, F. Seidel, Zell- und stoffwechselphysiologische untersuchungen an der wurzel von *Lemna minor* L. unter besonderer berücksichtigung von kalium- und kalziummangel, Planta 38 (1950) 431–473, https://doi.org/10.1007/BF01928941.
[64] M. Müller-Linow, J. Wilhelm, C. Briese, T. Wojciechowski, U. Schurr, F. Fiorani, Plant screen mobile: an open-source mobile device app for plant trait analysis, Plant Methods 15 (2019) 2, https://doi.org/10.1186/s13007-019-0386-z.
[65] Organization for Economic Co-operation and Development - OECD, Lemna sp. Growth inhibition test, Guidelines for the testing of chemicals. Updated Test Guideline 221 (2006).
[66] R.J. Strasser, A. Srivastava, M. Tsimilli-Michael, The fluorescence transient as a tool to characterize and screen photosynthetic samples, in: M. Yunus, U. Pathre, P. Mohanty (Eds.), Probing Photosynthesis: Mechanisms, Regulation and Adaptation, fisst ed., Taylor & Francis, London, 2000, pp. 445–483.
[67] A.R. Wellburn, The spectral determination of chlorophylls *a* and *b*, as well as total carotenoids, using various solvents with spectrophotometers of different resolution, J. Plant Physiol. 144 (1994) 307–313, https://doi.org/10.1016/S0176-1617(11)81192-2.
[68] M.M. Bradford, A rapid and sensitive method for the quantitation of microgram quantities of protein utilizing the principle of protein-dye binding, Anal. Biochem. 72 (1976) 248–254, https://doi.org/10.1016/j.cj.2017.04.003.
[69] A. Mátai, É. Hideg, A comparison of colorimetric assays detecting hydrogen peroxide in leaf extracts, Anal. Methods 9 (2017) 2357–2360, https://doi.org/10.1039/c7ay00126f.
[70] R.L. Heath, L. Packer, Photoperoxidation in isolated chloroplasts I. kinetics and stoichiometry of fatty acid peroxidation, Arch. Biochem. Biophys. 125 (1968) 189–198, https://doi.org/10.1016/0003-9861(68)90654-1.
[71] R.L. Levine, J.A. Williams, E.P. Stadtman, E. Shacter, Carbonyl assays for determination of oxidatively modified proteins, Methods Enzym. 233 (1994) 346–357, https://doi.org/10.1016/S0076-6879(94)33040-9.
[72] G. Colombo, M. Clerici, M.E. Garavaglia, D. Giustarini, R. Rossi, A. Milzani, I. Dalle-Donne, A step-by-step protocol for assaying protein carbonylation in biological samples, J. Chromatogr. B 1019 (2016) 178–190, https://doi.org/10.1016/j.jchromb.2015.11.052.
[73 N. Bauer, M. Tkalec, N. Major, A. Talanga Vasari, M. Tokić, S. Vitko, D. Ban, S. G. Ban, B. Salopek-Sondi, Mechanisms of kale (*Brassica oleracea* var. *acephala*) tolerance to individual and combined stresses of drought and elevated temperature, Int. J. Mol. Sci. 23 (2022), https://doi.org/10.3390/ijms231911494.
[74] C. Beauchamp, I. Fridovich, Superoxide dismutase: improved assays and an assay applicable to acrylamide gels, Anal. Biochem 44 (1971) 276–287, https://doi.org/10.1016/0003-2697(71)90370-8.
[75] H. Aebi, Catalase in vitro, Methods Enzym. (1984) 121–126, https://doi.org/10.1016/S0076-6879(84)05016-3.
[76] Y. Nakano, K. Asada, Hydrogen peroxide is scavenged by ascorbate-specific peroxidase in spinach chloroplasts, Plant Cell Physiol. 22 (1981) 867–880, https://doi.org/10.1093/oxfordjournals.pcp.a076232.
[77] J. Cohen, Statistical Power Analysis for the Behavioral Sciences, second ed, Routledge, New York, 1988, https://doi.org/10.4324/9780203771587.
[78] A.M.N.A.A. Rahman, A. Rusli, M.K. Abdullah, R.K. Shuib, Z.A.A. Hamid, K.M. Ku Ishak, M. Mohd Zaini Makhtar, M. Jaafar, M.D. Shafiq, A review of microplastic surface interactions in water and potential capturing methods, Water Sci. Engin (2024) 361–370, https://doi.org/10.1016/j.wse.2023.11.008.
[79] P. Wang, E. Lombi, S. Sun, K.G. Scheckel, A. Malysheva, B.A. McKenna, N. W. Menzies, F.J. Zhao, P.M. Kopittke, Characterizing the uptake, accumulation and toxicity of silver sulfide nanoparticles in plants, Environ. Sci. Nano 4 (2017) 448–460, https://doi.org/10.1039/c6en00489j.
[80] X.D. Sun, X.Z. Yuan, Y. Jia, L.J. Feng, F.P. Zhu, S.S. Dong, J. Liu, X. Kong, H. Tian, J.L. Duan, Z. Ding, S.G. Wang, B. Xing, Differentially charged nanoplastics demonstrate distinct accumulation in *Arabidopsis thaliana*, Nat. Nanotechnol. 15 (2020) 755–760, https://doi.org/10.1038/s41565-020-0707-4.
[81] C. Della Torre, E. Bergami, A. Salvati, C. Faleri, P. Cirino, K.A. Dawson, I. Corsi, Accumulation and embryotoxicity of polystyrene nanoparticles at early stage of development of sea urchin embryos *Paracentrotus lividus*, Environ. Sci. Technol. 48 (2014) 12302–12311, https://doi.org/10.1021/es502569w.
[82] S.E. Taylor, C.I. Pearce, K.A. Sanguinet, D. Hu, W.B. Chrisler, Y.M. Kim, Z. Wang, M. Flury, Polystyrene nano- and microplastic accumulation at Arabidopsis and wheat root cap cells, but no evidence for uptake into roots, Environ. Sci. Nano 7 (2020) 1942–1953, https://doi.org/10.1039/d0en00309c.
[83] M. Xu, F. Zhu, Y. Yang, M. Liu, X. Li, Y. Jiang, L. Feng, J. Duan, W. Wang, X. Yuan, X. Zhang, Mechanism of transport and toxicity response of *Chlorella sorokiniana* to polystyrene nanoplastics, Ecotoxicol. Environ. Saf. 270 (2024) 115901, https://doi.org/10.1016/j.ecoenv.2023.115901.
[84] C. Li, Y. Gao, S. He, H.Y. Chi, Z.C. Li, X.X. Zhou, B. Yan, Quantification of nanoplastic uptake in cucumber plants by pyrolysis gas chromatography/mass spectrometry, Environ. Sci. Technol. Lett. 8 (2021) 633–638, https://doi.org/10.1021/acs.estlett.1c00369.
[85] Z. Wang, S. Li, S. Jian, F. Ye, T. Wang, L. Gong, X. Li, Low temperature tolerance is impaired by polystyrene nanoplastics accumulated in cells of barley (*Hordeum vulgare* L.) plants, J. Hazard Mater. 426 (2022) 127826, https://doi.org/10.1016/j.jhazmat.2021.127826.
[86] Y. Dong, M. Gao, W. Qiu, Z. Song, Uptake of microplastics by carrots in presence of As (III): combined toxic effects, J. Hazard Mater. 411 (2021) 125055–125067, https://doi.org/10.1016/j.jhazmat.2021.125055.
[87] H. Sun, C. Lei, J. Xu, R. Li, Foliar uptake and leaf-to-root translocation of nanoplastics with different coating charge in maize plants, J. Hazard Mater. 416 (2021) 125854–125864, https://doi.org/10.1016/j.jhazmat.2021.125854.
[88] A. Avellan, J. Yun, Y. Zhang, E. Spielman-Sun, J.M. Unrine, J. Thieme, J. Li, E. Lombi, G. Bland, G.V. Lowry, Nanoparticle size and coating chemistry control foliar uptake pathways, translocation, and leaf-to-rhizosphere transport in wheat, ACS Nano 13 (2019) 5291–5305, https://doi.org/10.1021/acsnano.8b09781.
[89] E. Rouches, M.F. Dignac, S. Zhou, H. Carrere, Pyrolysis-GC–MS to assess the fungal pretreatment efficiency for wheat straw anaerobic digestion, J. Anal. Appl. Pyrolysis 123 (2017) 409–418, https://doi.org/10.1016/j.jaap.2016.10.012.
[90] L. Chen, X. Wang, H. Yang, Q. Lu, D. Li, Q. Yang, H. Chen, Study on pyrolysis behaviors of non-woody lignins with TG-FTIR and Py-GC/MS, J. Anal. Appl. Pyrolysis 113 (2015) 499–507, https://doi.org/10.1016/j.jaap.2015.03.018.
[91] X.-L. Cao, M. Sparling, L. Pelletier, R. Dabeka, Styrene in foods and dietary exposure estimates, Food Addit. Contam. Part A 35 (2018) 2045–2051, https://doi.org/10.1080/19440049.2018.1512760.
[92] Y. Díaz-de-Mera, A. Aranda, E. Martínez, A.A. Rodríguez, D. Rodríguez, A. Rodríguez, Formation of secondary aerosols from the ozonolysis of styrene: effect of SO_2 and H_2O, Atmos. Environ. 171 (2017) 25–31, https://doi.org/10.1016/j.atmosenv.2017.10.011.
[93] Z. Li, Q. Li, R. Li, J. Zhou, G. Wang, The distribution and impact of polystyrene nanoplastics on cucumber plants, Environ. Sci. Pollut. Res. 28 (2021) 16042–16053, https://doi.org/10.1007/s11356-020-11702-2.
[94] F. Xiao, L.-J. Feng, X.-D. Sun, Y. Wang, Z.-W. Wang, F.-P. Zhu, X.-Z. Yuan, Do polystyrene nanoplastics have similar effects on duckweed (*Lemna minor* L.) at environmentally relevant and observed-effect concentrations? Environ. Sci. Technol. 56 (2022) 4071–4079, https://doi.org/10.1021/acs.est.1c06595.
[95] H. Yu, X. Zhang, J. Hu, J. Peng, J. Qu, Ecotoxicity of polystyrene microplastics to submerged carnivorous *Utricularia vulgaris* plants in freshwater ecosystems, Environ. Pollut. 265 (2020) 114830, https://doi.org/10.1016/j.envpol.2020.114830.
[96] R. Ullah, M.T. Tsui, H. Chen, A. Chow, C. Williams, A. Ligaba-Osena, Microplastics interaction with terrestrial plants and their impacts on agriculture, J. Environ. Qual. 50 (2021) 1024–1041, https://doi.org/10.1002/jeq2.20264.
[97] L. Yin, X. Wen, D. Huang, C. Du, R. Deng, Z. Zhou, J. Tao, R. Li, W. Zhou, Z. Wang, H. Chen, Interactions between microplastics/nanoplastics and vascular plants, Environ. Pollut. 290 (2021) 117999, https://doi.org/10.1016/j.envpol.2021.117999.
[98] J. Lian, J. Wu, H. Xiong, A. Zeb, T. Yang, X. Su, L. Su, W. Liu, Impact of polystyrene nanoplastics (PSNPs) on seed germination and seedling growth of wheat (*Triticum aestivum* L.), J. Hazard Mater. 385 (2020) 121620, https://doi.org/10.1016/j.jhazmat.2019.121620.
[99] E. Agathokleous, Z. Feng, I. Iavicoli, E.J. Calabrese, The two faces of nanomaterials: a quantification of hormesis in algae and plants, Environ. Int. 131 (2019) 105044, https://doi.org/10.1016/j.envint.2019.105044.
[100] L. Yang, C. Ma, Toward a better understanding of microalgal photosynthesis in medium polluted with microplastics: a study of the radiative properties of microplastic particles, Front. Bioeng. Biotechnol. 11 (2023), https://doi.org/10.3389/fbioe.2023.1193033.
[101] H. Lepeduš, Ž. Vidaković-Cifrek, I. Šebalj, J. Antunović Dunić, V. Cesar, Effects of low and high irradiation levels on growth and PSII efficiency in *Lemna minor* L, Acta Bot. Croat. 79 (2020) 185–192, https://doi.org/10.37427/botcro-2020-016.
[102] C. Ozfidan-Konakci, E. Yildiztugay, B. Arikan, F.N. Alp-Turgut, M. Turan, H. Cavusoglu, H. Sakalak, Responses of individual and combined polystyrene and polymethyl methacrylate nanoplastics on hormonal content, fluorescence/photochemistry of chlorophylls and ROS scavenging capacity in *Lemna minor*

under arsenic-induced oxidative stress, Free Radic. Biol. Med. 196 (2023) 93–107, https://doi.org/10.1016/j.freeradbiomed.2023.01.015.
[103] B. Demmig-Adams, M. López-Pozo, S.K. Polutchko, P. Fourounjian, J.J. Stewart, M.C. Zenir, W.W. Adams, Growth and nutritional quality of lemnaceae viewed comparatively in an ecological and evolutionary context, Plants 11 (2022) 145–168, https://doi.org/10.3390/plants11020145.
[104] R. Therby-Vale, B. Lacombe, S.Y. Rhee, L. Nussaume, H. Rouached, Mineral nutrient signaling controls photosynthesis: focus on iron deficiency-induced chlorosis, Trends Plant. Sci. 27 (2022) 502–509, https://doi.org/10.1016/j.tplants.2021.11.005.
[105] P. Wang, B. Grimm, Connecting chlorophyll metabolism with accumulation of the photosynthetic apparatus, Trends Plant. Sci. 26 (2021) 484–495, https://doi.org/10.1016/j.tplants.2020.12.005.
[106] L. Teng, Y. Zhu, H. Li, X. Song, L. Shi, The phytotoxicity of microplastics to the photosynthetic performance and transcriptome profiling of *Nicotiana tabacum* seedlings, Ecotoxicol. Environ. Saf. 231 (2022) 113155, https://doi.org/10.1016/j.ecoenv.2021.113155.
[107] L. Xu, Z. Chu, X. Li, C. Feng, Y. Zhang, C. Wang, J. Zhang, C. Xu, J. Wang, H. Tang, Proteomic insights into composition-dependent effects of microplastics on freshwater microalgae *Chlamydomonas reinhardtii*, Environ. Sci. Nano 11 (2024) 3440–3456, https://doi.org/10.1039/D4EN00300D.
[108] X. Li, Z. Chu, C. Feng, P. Song, T. Yang, L. Zhou, X. Zhao, X. Chai, J. Xing, S. Chen, J. Zhang, J. Wang, G. Liu, H. Tang, Unveiling the molecular mechanisms of size-dependent effect of polystyrene micro/nano-plastics on *Chlamydomonas reinhardtii* through proteomic profiling, Chemosphere 358 (2024) 142220, https://doi.org/10.1016/j.chemosphere.2024.142220.
[109] A. Kumari, V.D. Rajput, S.S. Mandzhieva, S. Rajput, T. Minkina, R. Kaur, S. Sushkova, P. Kumari, A. Ranjan, V.P. Kalinitchenko, A.P. Glinushkin, Microplastic pollution: an emerging threat to terrestrial plants and insights into its remediation strategies, Plants 11 (2022) 340.
[110] A. Parvaiz, C.A. Jaleel, M.A. Salem, G. Nabi, S. Sharma, Roles of enzymatic and nonenzymatic antioxidants in plants during abiotic stress, Crit. Rev. Biotechnol. 30 (2010) 161–175, https://doi.org/10.3109/07388550903524243.
[111] F. Nazir, Q. Fariduddin, T.A. Khan, Hydrogen peroxide as a signalling molecule in plants and its crosstalk with other plant growth regulators under heavy metal stress, Chemosphere 252 (2020) 126486, https://doi.org/10.1016/j.chemosphere.2020.126486.
[112] H. Claeys, S. Van Landeghem, M. Dubois, K. Maleux, D. Inzé, What is stress? Dose-response effects in commonly used in vitro stress assays, Plant Physiol. 165 (2014) 519–527, https://doi.org/10.1104/pp.113.234641.
[113] H. Yu, J. Peng, X. Cao, Y. Wang, Z. Zhang, Y. Xu, W. Qi, Effects of microplastics and glyphosate on growth rate, morphological plasticity, photosynthesis, and oxidative stress in the aquatic species *Salvinia cucullata*, Environ. Pollut. 279 (2021) 116900–116909, https://doi.org/10.1016/j.envpol.2021.116900.
[114] G. Li, C. Qiu, D. Zhang, M. Lv, X. Liao, Q. Li, L. Wang, Effects of polystyrene nanoplastics (PSNPs) on the physiology of *Allium sativum* L.: photosynthetic pigments, antioxidant enzymes, phytohormones, and nutritional quality, Environ. Exp. Bot. 219 (2024) 105654, https://doi.org/10.1016/j.envexpbot.2024.105654.
[115] S. Maity, A. Chatterjee, R. Guchhait, S. De, K. Pramanick, Cytogenotoxic potential of a hazardous material, polystyrene microparticles on *Allium cepa* L, J. Hazard Mater. 385 (2020) 121560–121587, https://doi.org/10.1016/j.jhazmat.2019.121560.
[116] Z. Li, R. Li, Q. Li, J. Zhou, G. Wang, Physiological response of cucumber (*Cucumis sativus* L.) leaves to polystyrene nanoplastics pollution, Chemosphere 255 (2020) 127041–127051, https://doi.org/10.1016/j.chemosphere.2020.127041.
[117] J. Li, S. Yu, Y. Yu, M. Xu, Effects of microplastics on higher plants: a review, Bull. Environ. Contam. Toxicol. 109 (2022) 241–265, https://doi.org/10.1007/s00128-022-03566-8.
[118] A. Yan, Z. Chen, Impacts of silver nanoparticles on plants: a focus on the phytotoxicity and underlying mechanism, Int. J. Mol. Sci. 20 (2019) 23–25, https://doi.org/10.3390/ijms20051003.
[119] S. Bauduin, M. Latini, I. Belleggia, M. Migliore, M. Biancucci, R. Mattioli, A. Francioso, L. Mosca, D. Funck, M. Trovato, Interplay between proline metabolism and ROS in the fine tuning of root-meristem size in *Arabidopsis*, Plants 11 (2022) 1512–1535, https://doi.org/10.3390/plants11111512.
[120] X. Liang, L. Zhang, S.K. Natarajan, D.F. Becker, Proline mechanisms of stress survival, Antioxid. Redox Signal 19 (2013) 998–1011, https://doi.org/10.1089/ars.2012.5074.
[121] A. Waśkiewicz, M. Beszterda, P. Goliński, Nonenzymatic antioxidants in plants, in: A. Parvaiz (Ed.), Oxidative damage to plants, Elsevier, Amsterdam, Netherlands, 2014, pp. 201–234, https://doi.org/10.1016/B978-0-12-799963-0.00007-1.
[122] F.A. Gondim, E. Gomes-Filho, J.H. Costa, N.L. Mendes Alencar, J.T. Prisco, Catalase plays a key role in salt stress acclimation induced by hydrogen peroxide pretreatment in maize, Plant Physiol. Biochem 56 (2012) 62–71, https://doi.org/10.1016/j.plaphy.2012.04.012.
[123] G. Polo, F. Lionetto, M.E. Giordano, M.G. Lionetto, Interaction of micro- and nanoplastics with enzymes: the case of carbonic anhydrase, Int. J. Mol. Sci. 25 (2024) 9716, https://doi.org/10.3390/ijms25179716.
[124] C.Q. Zhou, C.H. Lu, L. Mai, L.J. Bao, L.Y. Liu, E.Y. Zeng, Response of rice (*Oryza sativa* L.) roots to nanoplastic treatment at seedling stage, J. Hazard Mater. 401 (2021) 123412–123422, https://doi.org/10.1016/j.jhazmat.2020.123412.
[125] Q. Zhang, M. Zhao, F. Meng, Y. Xiao, W. Dai, Y. Luan, Effect of polystyrene microplastics on rice seed germination and antioxidant enzyme activity, Toxics 9 (2021) 179–198, https://doi.org/10.3390/toxics9080179.
[126] D. An, J. Na, J. Song, J. Jung, Size-dependent chronic toxicity of fragmented polyethylene microplastics to *Daphnia magna*, Chemosphere 271 (2021) 129591, https://doi.org/10.1016/j.chemosphere.2021.129591.
[127] X. Li, Y. Chen, S. Zhang, Y. Dong, Q. Pang, I. Lynch, C. Xie, Z. Guo, P. Zhang, From marine to freshwater environment: a review of the ecotoxicological effects of microplastics, Ecotoxicol. Environ. Saf. 251 (2023) 114564, https://doi.org/10.1016/j.ecoenv.2023.114564.
[128] T.H. Nguyen, T.-C. Kieu-Le, F.H.M. Tang, F. Maggi, Controlling factors of microplastic fibre settling through a water column, Sci. Total Environ. 838 (2022) 156011, https://doi.org/10.1016/j.scitotenv.2022.156011.
[129] J.-S. Park, J.-W. Yoo, Y.-H. Lee, C. Park, Y.-M. Lee, Size- and shape-dependent ingestion and acute toxicity of fragmented and spherical microplastics in the absence and presence of prey on two marine zooplankton, Mar. Pollut. Bull. 206 (2024) 116768, https://doi.org/10.1016/j.marpolbul.2024.116768.
[130] B. Klun, U. Rozman, M. Ogrizek, G. Kalčíková, The first plastic produced, but the latest studied in microplastics research: the assessment of leaching, ecotoxicity and bioadhesion of Bakelite microplastics, Environ. Pollut. 307 (2022) 119454, https://doi.org/10.1016/j.envpol.2022.119454.
[131] A.T.N. Do, Y. Ha, J.-H. Kwon, Leaching of microplastic-associated additives in aquatic environments: a critical review, Environ. Pollut. 305 (2022) 119258, https://doi.org/10.1016/j.envpol.2022.119258.
[132] A. Jemec Kokalj, D. Kuehnel, B. Puntar, A. Žgajnar Gotvajn, G. Kalčikova, An exploratory ecotoxicity study of primary microplastics versus aged in natural waters and wastewaters, Environ. Pollut. 254 (2019) 112980, https://doi.org/10.1016/j.envpol.2019.112980.
[133] S. Gao, G. Huang, D. Han, Ecotoxicity of plastic leachates on aquatic plants: multi-factor multi-effect meta-analysis, Water Res 268 (2025) 122577, https://doi.org/10.1016/j.watres.2024.122577.
[134] C. Chen, R. Du, J. Tang, B. Wang, F. Li, Z. Zhang, G. Yu, Characterization of microplastic-derived dissolved organic matter in freshwater: effects of light irradiation and polymer types, Environ. Int. 185 (2024) 108536, https://doi.org/10.1016/j.envint.2024.108536.
[135] N.R. Maddela, D. Kakarla, K. Venkateswarlu, M. Megharaj, Additives of plastics: entry into the environment and potential risks to human and ecological health, J. Environ. Manag. 348 (2023) 119364, https://doi.org/10.1016/j.jenvman.2023.119364.
[136] P. Burić, I. Kovačić, L. Jurković, S. Tez, R. Oral, N. Landeka, D.M. Lyons, Polymer chemical identity as a key factor in microplastic–insecticide antagonistic effects during embryogenesis of sea urchin *Arbacia lixula*, Int. J. Mol. Sci. 24 (2023) 4136, https://doi.org/10.3390/ijms24044136.